

UC San Diego

UC San Diego Electronic Theses and Dissertations

Title

Identification of Rab11 as a target of edema factor and dominant-negative mutants of anthrax lethal factor

Permalink

<https://escholarship.org/uc/item/8h02532t>

Author

Kurkciyan, Adrienne A.

Publication Date

2013

Peer reviewed|Thesis/dissertation

UNIVERSITY OF CALIFORNIA, SAN DIEGO

Identification of Rab11 as a target of edema factor and dominant-negative
mutants of anthrax lethal factor

A thesis submitted in partial satisfaction of the
requirements for the degree Master of Science

in

Biology

by

Adrianne A. Kurkciyan

Committee in Charge:

Professor Ethan Bier, Chair
Professor Amy Kiger
Professor Kit Pogliano

2013

Copyright

Adrianne A. Kurkciyan, 2013

All rights reserved.

The Thesis of Adrienne A. Kurkciyan is approved, and it is
acceptable in quality and form for publication of microfilm and electronically:

Chair

University of California, San Diego

2013

Table of Contents

Signature Page.....	iii
Table of Contents.....	iv
List of Figures.....	v
List of Supplemental Tables.....	vi
Acknowledgements.....	vii
Abstract.....	ix
Introduction	1
I The search for anthrax toxin effectors using genetic screens.....	12
Results.....	13
Discussion.....	25
II The generation and analysis of dominant negative mutants for lethal factor....	32
Results.....	33
Discussion.....	41
Materials and Methods.....	43
Supplementary Tables.....	46
References.....	52

List of Figures

Figure 1 - “Anthrax toxins: entry into host cells and mechanism of action”	5
Figure 2 - Wing phenotypes indicate an interaction between EF and Rab11.....	14
Figure 3 - EF and LF converge at the Rab11/Sec15 exocyst to disrupt Delta and DECad expression at the AJ.....	15
Figure 4 - Decreasing expression of Sec15, Sec5, and Exo70 strengthens the LF phenotype.....	19
Figure 5 - CG5745 ^{RNAi} and CG17282 ^{RNAi} increase the strength of the EF and LF phenotype.....	21
Figure 6 - Loss of CG5745 and CG17282 disrupts levels of exocyst partners Sec15 and Rab11 in a similar fashion.....	24
Figure 7 - <i>LF_T</i> and <i>EF_T</i> transgenic fly lines.....	34
Figure 8 - Δ2,3 screen generates two dominant negatives against LF.....	37
Figure 9 – Analysis of LF _T DN1 and LF _T DN2.....	39

List of Supplemental Tables

Supplemental Table 1 - Effects of expressing dominant negative Rabs (RabDN) in the wing and the effects of wild-type Rabs (RabWT) on EF phenotype.....	46
Supplemental Table 2 - Wing phenotypes of expressing RNAi lines and effects on EF and LF.....	47

Acknowledgements

I would like to express my appreciation to Dr. Ethan Bier, for the opportunity to learn from his lab and advising me in my research. He has always been kind and supportive. His passion for science inspires and motivates me.

I would like to thank Dr. Amy Kiger and Dr. Kit Pogliano, for being on my committee.

I am grateful for having Dr. Annabel Guichard as a mentor. From teaching me lab techniques during the beginning to providing comments on my thesis at the very end, she always extended her help openly. I would also like to thank Beatriz Cruz-Moreno, for her help in mentoring me.

I would also like to thank all members of the Bier lab, both past and present, including: Valentino Gantz, Francisco Esteves, Orna Cook, Margerie Smelkinson, Long Do, and Tamar Grossman, for their assistance time to time and companionship. My research experience here would not have been the same without the work environment they helped create.

To the two people I can never thank enough: my parents. You have taught me more lessons than any level of schooling could, and have made me into the person I am today.

I would also like to acknowledge the use of previously published material, which has been done with permission. Figure 1, in the introduction, comes from the following review:

Guichard, A., Nizet, V. & Bier, E. New insights into the biological effects of anthrax toxins: linking cellular to organismal responses. *Microbes Infect.* **14**, 97–118 (2012).

Images used in Figure 3, comes from work done by Annabel Guichard and Beatriz Cruz-Moreno. Most of these images have been published in the following article:

Guichard, A., McGillivray, S. M., Cruz-Moreno, B., van Sorge, N. M., Nizet, V. & Bier, E. Anthrax toxins cooperatively inhibit endocytic recycling by the Rab11/Sec15 exocyst. *Nature* **467**, 854–858 (2010).

ABSTRACT OF THE THESIS

Identification of Rab11 as a target of edema factor and dominant-negative mutants of anthrax lethal factor

by

Adrianne A. Kurkciyan

Master of Science in Biology

University of California, San Diego, 2013

Professor Ethan Bier, Chair

Anthrax is a fatal disease caused by the spore-formulating bacterium, *Bacillus anthracis*. The potential for anthrax as a bioterrorist weapon raises concern, and is still common in the developing world. Antibiotic treatment of anthrax is often not effective, because toxins released in the host bloodstream can cause death even after clearance of the bacterium. Thus, it is important to

further develop our knowledge of how anthrax causes its deadly effects as well as develop treatments targeting the toxins themselves.

The anthrax toxin edema factor (EF) is a calmodulin-dependent adenylate cyclase and lethal factor (LF) is a zinc metalloprotease, which cleaves and inactivates MAPKKs. Like many other bacterial toxins, their activity targets conserved cellular components, making it possible to study their activity using an invertebrate model such as *Drosophila*.

Using *UAS-EF* and *UAS-LF* transgenic lines, an extensive interaction screen with candidate UAS lines was used to identify novel targets for toxin activity. EF and LF showed synergistic interaction with Rab11 GTPase, a recycling endosome regulator, and its exocyst binding partner Sec15. Also, loss of other exocyst components Sec5, Sec15, and Exo70 enhanced the severity of the LF phenotype. Two other candidates, CG5745 and CG17282, disrupt the exocyst through their action on Sec15 and possibly Rab11. Increased knowledge of toxin activity in the long run may prove to be useful in rational drug design. Furthermore, as a more direct approach to treatment development, I conducted a genetic screen, which generated two dominant negative mutants of lethal factor.

Introduction

Overview of Anthrax Disease

Anthrax is a disease primarily affecting livestock. Therefore, concern over anthrax has long been for these agricultural animals and the people who work with them^{1,2}. With advances in veterinary practices the disease has become rare in the Western world³. Incidences such as the stockpiling of anthrax by terror-oriented regimes, post-9/11 fears, and the 2001 anthrax mail scare brought attention back to anthrax, which has a strong potential as a bioterrorist weapon due to the resiliency of its spores, the ease of aerosolizing spores for mass inhalation, and the lethality of the disease^{4,5}. This changed the dynamics of how we look at anthrax and developed a need to prepare for potential attacks, increasing interest to expand our knowledge and develop treatments for the disease.

Exposure to anthrax can occur through skin abrasion, ingestion, or inhalation, leading to the cutaneous, inhalational, or gastrointestinal forms of the disease, respectively. The cutaneous form is the least severe of the three forms as it is usually maintained in the dermis. It is characterized by edema that progress to painless sores that later form large, coal-black scars. Unfortunately, up to 20% of cutaneous infections lead to systemic infection like inhalational and gastrointestinal anthrax, which is often fatal^{6,7}. Due to recent incidences of infection amongst IV drug users, a new category, “subcutaneous” anthrax, has begun to emerge⁸⁻¹⁰.

In addition to being better prepared against a bioterrorism attack, anthrax and anthrax treatment research will be of benefit to populations where the disease is more common due to poor agricultural vaccine and hygiene practices. Recent anthrax outbreaks include Zambia (2011), Bengal (2010), and Zimbabwe (2007)^{7,11,12}. A review of reports in more developed countries like Turkey also show 2210 recorded cases between the years 2000-2005¹³. This of course is the number for recorded cases; actual case numbers are likely to be greater. Furthermore, incidences of anthrax occurring in IV drug users in the UK and Germany is a case in point that even developed countries are susceptible to spontaneous outbreaks⁸⁻¹⁰.

Systemic Infection: Prodromal and Fulminant Stages

Systemic anthrax occurs in two different stages: the asymptomatic prodromal phase and the fulminant phase. The prodromal phase usually lasts 2-4 days, during which time the anthrax toxins lethal toxin (LT) and edema toxin (ET) primarily target the immune system. The toxins alter chemotaxis and migration of immune cells and reduce overall cytokine production. Phagocytic myeloid cells engulf bacterial spores and transport them to lymph nodes where they undergo apoptosis, releasing spores that germinate to vegetative bacteria (reviewed in ⁶). Thus, in the case of inhalation anthrax, the host's immune system essentially helps spread the disease. This subversion of the immune system helps establish infection throughout the body, facilitating entry into the fulminant phase.

At the onset of the fulminant stage, patients report with symptoms such as cough, fatigue, nausea, and shortness of breath¹⁴. During this stage bacteria proliferate and continue to spread to organs via blood. As the anthrax target receptors tumor endothelial marker (TEM8) and capillary morphogenesis gene 2 (CMG2) are highly and broadly expressed, many tissue types are subject to attack by the toxins¹⁵. Organs affected include mediastinal lymph nodes, lung, heart, kidneys, liver, gastrointestinal tract, and meninges. The fulminant stage progresses so rapidly, that it usually causes death within 1-4 days^{14,16}.

One of the effects of these toxins is to increase endothelial permeability^{17,18}, easing dissemination of *B. anthracis* to organs of the body. As an example, this increased permeability even compromises the blood brain barrier, with data showing meningitis in ~50% of human patients infected with systemic anthrax¹⁶. Increased endothelial permeability also causes vascular leakage, causing edema, including heart and pericardial edema^{17,18}.

One study took advantage of the transparent bodies of zebrafish embryos to show the progression of LT effects on the cardiovascularity *in vivo*. They showed a dose-dependent phenotype of vasculature defects, which led to fluid accumulation in the heart. Severe cases even led to a cessation of blood flow as the blood got trapped within the heart chambers¹⁸.

In addition to heart problems resulting from compromised vasculature, toxins target cardiac tissue directly as well. LT treatment in mice increases cardiac damage biomarkers and causes swelling and degeneration of the cardiac endothelium, defects of the mitochondria and sarcoplasmic reticulum, and

myofilament fragmentation and necrosis¹⁹. LT treatment of rabbits has also confirmed direct damage to cardiac tissue²⁰. ET in mice causes cardiac lesions, myofiber separation, cardiomyocyte degeneration, and eventually necrosis²¹. These effects on the cardiovascular system culminate into toxic shock-like symptoms, which is the usual cause of death by anthrax⁶.

Cell Entry and Basic Biochemistry of Anthrax Toxins

Bacillus anthracis is the Gram-positive, sporulating bacterium causing anthrax²². It relies on plasmids pXO2 and pXO1 for its pathogenic activity. These are responsible for the formation of *B. anthracis*' inert poly- γ -D-glutamyl capsule and the production of a tripartite A/B type exotoxin, respectively^{23–25}.

The exotoxin's B component, protective antigen (PA), shuttles in the toxic A components, edema factor (EF) and lethal factor (LF), inside the cell (Fig. 1). PA is synthesized as a precursor that binds to the highly expressed cell surface receptors TEM8 and CMG2^{26,27}. After proteolytic cleavage by furin the active 63 kDa PA products oligomerize to form a heptameric ring binding three units of EF and/or LF^{28–32}. This complex is endocytosed via clathrin-mediated endocytosis³³. A pH drop in early endosomes causes the PA heptamer to form a pore out of which EF and LF are translocated to the cytoplasm after they reach the late endosomes^{30,34–36}. EF remains associated with membranes of the late endosome, while LF disperses in the cytosol^{37,38} (Fig. 1).

EF is a potent, calmodulin (CaM)-dependent adenylate cyclase (AC)³⁹. EF has 3 domains: a PA-binding N-terminal domain highly related to the PA-binding

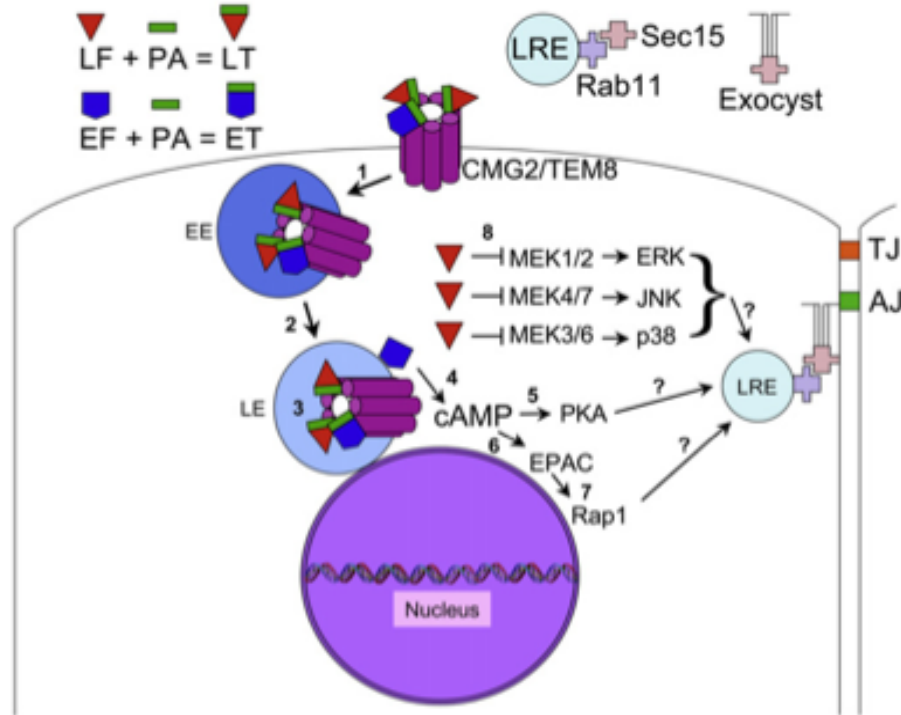


Figure 1: “Anthrax toxins: entry into host cells and mechanism of action.”

1) PA binds to the receptors CMG2 or TEM8. Proteolytic cleavage by furin activates PA, which then associates with EF and LF to form a complex consisting of 3 PA/EF or PA/LF. This complex is endocytosed and trafficked from 2) early endosomes (EE) to 3) late endosomes (LE) 4) where they are translocated into the cytosol. EF remains associated with the late endosomal membrane, surrounding the nucleus. EF is a potent CaM-dependent AC, resulting in high levels of cAMP 5) effecting cAMP targets such as PKA and 6) EPAC. 8) LF is a zinc metalloprotease that cleaves MAPKKs (MEKs). Figure taken from Bier, et al⁶, with permission.

domain of LF, a catalytic domain, and a helical C-terminal domain which inhibits the catalytic domain in the absence of CaM (reviewed in ⁴⁰). As noted above, EF remains associated with the membranes of the late endosome, which surrounds the nucleus^{37,38}. As a result, EF generates a cAMP gradient with levels highest near the nucleus and decreasing towards the plasma membrane, which is opposite to the endogenous levels of the host cell. In addition, EF is much more

potent than endogenous AC^{6,41}. These elevated levels cause an unregulated activation of cAMP targets such as protein kinase A (PKA) and exchange protein directly activated by cAMP (Epac), a guanine nucleotide exchange factor (GEF) specific for Rap GTPases^{42,43}.

LF is a zinc metalloprotease that inactivates most members of the MAPKK family by cleaving within the N-terminus domain, thus rendering MAPKK unable to interact with its MAPK substrates^{44–46}. Inactivation of MAPKKs disrupts activation of the Erk1/2, JNK, and p38 signaling pathways⁴⁷ (Fig. 1). LF is composed of 4 domains. Domain I is the N-terminal, PA-binding domain. Domains II-IV all bind to MAPKK. Domain III is a helical domain that gives specificity towards the MAPKK substrate. Domain IV is the catalytic domain that cleaves the substrate^{48,49}.

Much has been learned about the individual molecular actions of LF and EF, but previous studies have shown evidence they act synergistically as well. Stanley and Smith provided the earliest evidence of synergism when they showed extracts of ET (EF+PA) + LT (LF+PA) induce greater lethality than what would be expected if their individual effects were additive⁵⁰. In another study using modified strains of *B. anthracis*, infection of mice by an EF⁻ strain was lethal but did not produce edema, whereas LF⁻ strains produced edema but were not lethal. However, infection by Sterne strain 7702 (containing all three toxin components), was more lethal than the EF⁻ strain and produced greater edema than LF⁻ strains, providing further evidence over the synergism between the two toxins⁵¹.

Current Treatments for Anthrax

One of the most pivotal advancements of clinical microbiology is the first successful vaccination of livestock by Louis Pasteur against anthrax¹. At the time, the incidence of anthrax among agricultural workers was all too common. In today's Western world, the disease has become rare due to the regular vaccination of livestock and advancements in hygiene. Vaccines have also been developed fit for human use, but due to the rarity of the disease only high-risk groups are vaccinated (reviewed in ³).

All current vaccines contain PA, as it is highly immunogenic and a non-toxic subunit of the toxin^{3,52}. Also, since anti-PA antibodies neutralize PA they prevent onset of the disease. However, PA-based vaccines have their limitations. Immune memory elicited by PA does not last long, and repeated administration is needed. Live vaccines, have higher efficacy but are not considered fit for human use. Vaccine research continues with different adjuvants and other modifications to develop the next generation of anthrax vaccines³.

In situations when anthrax exposure is known, immediate treatment should be started. For these cases, the use of antibiotics alone may be insufficient as they only work on germinated bacteria. Resistant spores that germinate after cessation of antibiotic treatment reinfect the individual. Research in guinea pigs has shown adding a PA-based vaccine to the antibiotic treatment prevents reinfection⁵³.

With unknown exposure, humans infected with anthrax usually seek medical attention during the fulminant stage when symptoms begin to manifest.

Unfortunately by this time, the toxins are present at elevated levels and killing the bacteria with antibiotics is usually not sufficient to save the patient^{6,54}. Therefore, developing treatments that neutralize the toxins themselves is an essential strategy for establishing an effective anthrax treatment. Toxin-targeting drugs would also be critical for the treatment of antibiotic-resistant strains. To address this issue, one segment of my research involved the making of dominant negative (DN) versions of LF and EF, with the goal of generating a product that can target toxins directly.

***Drosophila melanogaster* as a model organism**

Due to its relatively quick generation time, sequenced genome, and cost efficiency, *Drosophila melanogaster* has proved itself to be an ideal model organism in many laboratory settings⁵⁵. As many bacterial and viral pathogens target conserved pathways, *D. melanogaster* can be a potential model for the study of human infectious diseases. In our lab, we have demonstrated its usefulness in the study of anthrax as well as cholera and influenza.

The GAL4/UAS system is an indispensable genetic tool for *Drosophila* research, used to develop transgenic flies expressing a gene of interest. This is a two-part system. The yeast Upstream Activation Sequence (UAS) is used as an enhancer for the gene of interest, which is regulated by the yeast transcriptional activator GAL4⁵⁶. There exist many lines of GAL4, each having expression patterns in specific tissues. Transgenic fly lines are usually made without a GAL4 insertion, so that the flies do not express the gene unless they are crossed to a

GAL4 line. This provides the control over where and when the desired gene gets expressed.

Characterization of Anthrax Toxins Lethal Factor and Edema Factor in *Drosophila*⁵⁷

Members of the Bier and Karin lab verified *D. melanogaster* can be a model organism for anthrax disease in humans by showing LF and EF target fly homologs of known vertebrate targets. The GAL4/UAS system was used to develop *UAS-LF* and *UAS-EF* fly lines for this study. By expressing the toxins directly in the cells, the need for PA-mediated endocytosis is bypassed. Therefore, studies using this method are limited to toxin action within the cell.

As MAPKKs are targets for LF, the four known *Drosophila* MAPKKs were checked as targets. They were found to have matches with a consensus amino acid sequence for known N-terminal cleavage sites of six different human MAPKKs. LF cleaved the *Drosophila* MAPKKs, Hemipterous (Hep), Licorne (Lic), and possibly Dsor1, *in vitro*. Epistasis experiments showed LF is capable of *in vivo* activity as well. LF expression causes a disruption of the c-Jun N-terminal kinase (JNK) signaling pathway, which acts downstream of Hep. This was indicated by a variety of phenotypes consistent with disruption of the Hep/JNK signaling pathway including: disrupted dorsal closure and a reduction of the JNK target gene *decapentaplegic (dpp)* in embryos, disrupted closure in the adult thorax, and partial loss of the fifth vein in wings. LF inhibits the RTK/Ras/Dsor/MAPK pathway as well. LF expression in the wing produces a

phenotype of small, elongated scooped wings (Fig. 7c). Similar phenotypes emerge with dominant negative (DN) genes of RTK/Ras/Dsor/MAPK pathway components. Other supporting data for disruption of Dsor includes the increased intensity with expressing LF in loss of function *Dsor*⁻ backgrounds. Furthermore, LF decreases the *in situ* activation of MAPK, showing that LF acts upstream of MAPK.

Expression of EF in the wing by dppG4 produces a phenotype consistent with a disrupted *hedgehog* (*hh*) pathway. As cAMP-dependent PKA inhibits this pathway, it is expected that EF causes inhibition of *hh* signaling as a result of elevated cAMP levels. The regulatory subunit of PKA (PKAr) inhibits the catalytic subunit of PKA (PKAc). Expression of PKAr therefore promotes *Hh* signaling, causing a broadened wing and lethality. This is reversed by EF expression, further confirming EF acts at the level of *Hh* signaling.

These results show that the toxic effects of LF and EF are effective against conserved signaling components MAPKKs and cAMP target PKA in the *D. melanogaster* system, setting the stage for further studies analyzing the activities of the anthrax toxins.

Edema Factor and Lethal Factor synergize to inhibit the Notch pathway

After establishing *D. melanogaster* as a model organism for studying anthrax at the cellular level, the Bier lab began using *Drosophila* to study the cellular effects of EF and LF, using the developing wing as a well characterized model system. Expression of EF and LF, using a variety of wing GAL4 drivers,

produced wing phenotypes typical of Notch mutants, including wing notching and thickened veins¹⁷. Highly conserved among metazoans, the Notch pathway is important for cell-cell communication and regulates processes such as cell differentiation, cell proliferation, and cell death⁵⁸. In the imaginal wing disc, high-level expression of either toxin reduced levels of Notch target genes *wingless* (*wg*) and *cut*, consistent with the idea that they inhibit Notch signaling. LF and EF expression also affected expression of the Notch ligand Delta (DI), which instead of accumulating at the apical junctions, was found in large misshapen intracellular vesicles. Furthermore, EF reduced levels of another Notch ligand, Serrate¹⁷. When expressed together using a weak wing GAL4 driver (1348), or a strong wing GAL4 driver (MS1096, herein referred to as *wngG4*), EF and LF led to much stronger phenotypes than when either toxin was expressed alone. Similarly in wing discs, coexpression of EF and LF led to a stronger reduction of *wg* than either toxin expressed alone¹⁷. These results, consistent with previous studies indicating toxin synergy^{50,51}, point to the Notch signaling pathway as the point of synergy.

I

The search for anthrax toxin effectors using genetic screens

Results

EF and LF converge at the Rab11/Sec15 exocyst to disrupt trafficking to the AJ

As noted previously, LF and EF expression in the wing discs reduced levels of DI at the apical surface. A possible explanation was that the toxins inhibit trafficking of DI to the apical surface, possibly by affecting the endocytosis and recycling process that normally targets DI to the adherens junction (AJ)^{17,59}. To address this question, I initiated a genetic screen, aimed to define which step of DI endocytic trafficking was interrupted by EF and LF. Small GTPases from the Rab family regulate specific steps in membrane trafficking⁶⁰, and were therefore prime candidates for being disrupted by anthrax toxins.

I used dominant negative (DN) and wild-type (WT) versions from all available transgenic Rabs lines⁶¹, and expressed them at high levels in the developing wings (using *wngGAL4*) either alone or with EF. Due to time constraints and previous results suggesting EF was more likely to have a detectable effect, LF was only co-expressed with the more well-known Rabs 4, 5, 7, and 11.

The most striking results came from Rab11, which is involved in regulating the recycling endosome⁶⁰. Rab11(DN) produced a phenotype nearly identical to EF and when co-expressed with either EF or LF, synergized to produce a stronger phenotype (Fig. 2a-c,f), consistent with disruption of Rab11 causing Notch inhibitory effects. Rab11(WT), which produced no phenotype on its own, suppressed the EF phenotype (Fig. 2d,e).

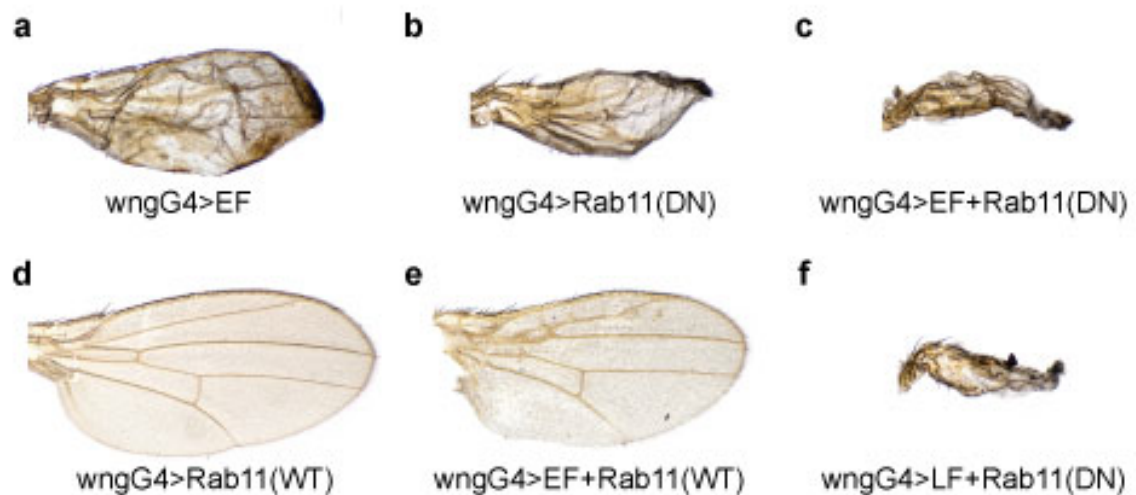


Figure 2: Wing phenotypes indicate an interaction between EF and Rab11.

b, Expressing Rab11(DN) in the wing mimics the **a**, EF phenotype. Rab11(DN) synergizes with **c**, EF and **f**, LF. **d**, Rab11WT, which has no phenotype on its own, **e**, rescues the wing from EF.

My colleagues, Annabel Guichard and Beatriz Cruz-Moreno, further investigated this finding. Rab11(DN) was found to act similarly to EF in blocking DL trafficking to the cell surface (Fig. 3a-c). It was also found that the Rab11 GTPase in wing discs, which is normally distributed as small grainy particles on the apical surface, was greatly reduced when co-expressed with EF, but not LF. Instead, in *EF*-expressing discs, Rab11 abnormally appeared in basolateral areas of the wing disc (Fig. 3d-f). These data suggest EF reduces and/or alters the distribution of Rab 11 GTPase. Levels of DE-Cadherin (DECad), an adhesion molecule that colocalizes with Delta, was greatly reduced by EF and Rab11(DN) (Fig. 3g-h). Co-expression of Rab11(WT) partially rescued this down-regulation of DeCad (data not shown). Expression of other AJ proteins were only slightly

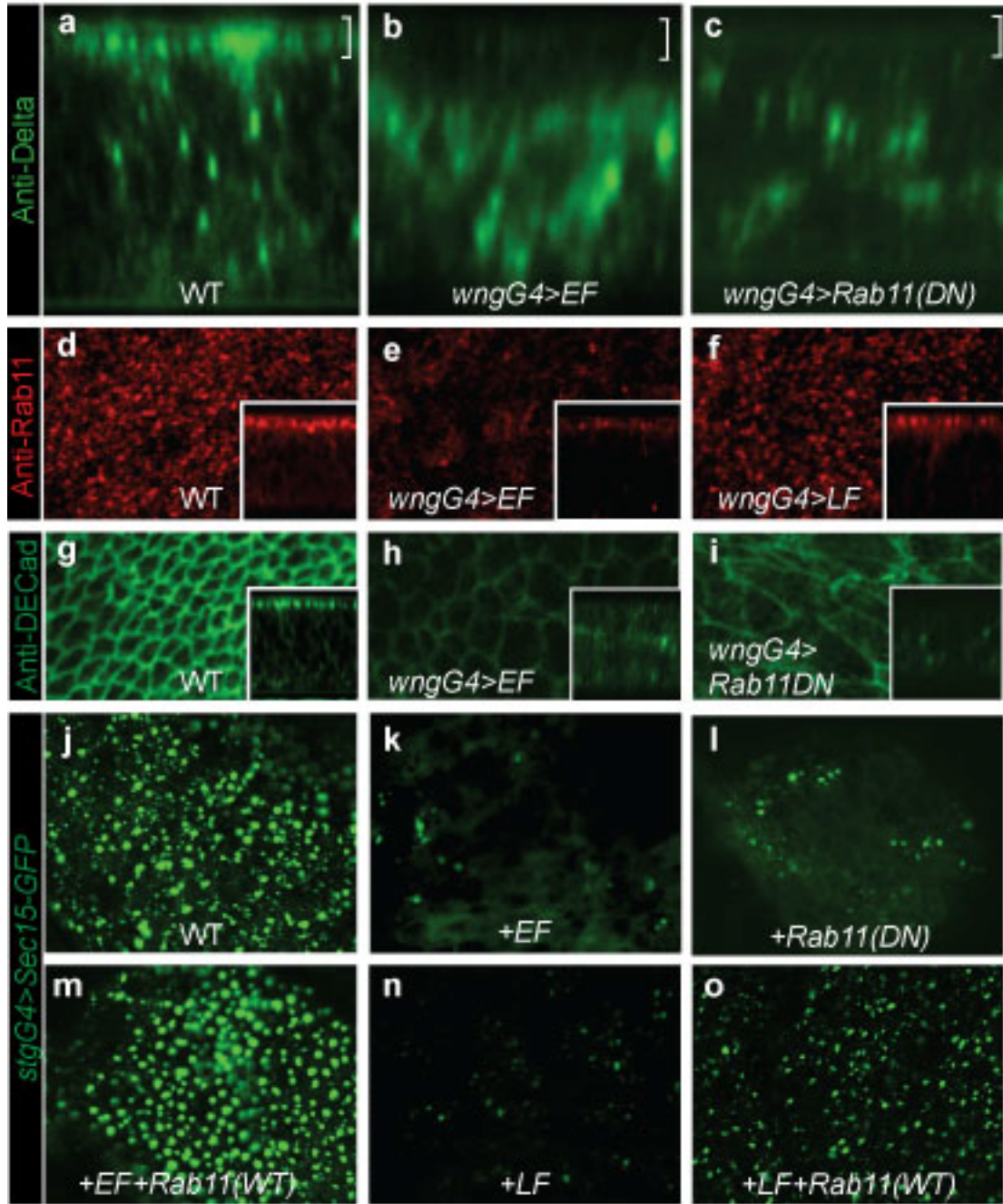


Figure 3: EF and LF converge at the Rab11/Sec15 exocyst to disrupt Delta and DEcad expression at the AJ. **a-c**, Z-sections of DI expression in the wing disc. **a**, In the WT disc, DI is expressed in both the cell surface (bracket) and intracellularly. In **e**, and **f**, DI expression is diminished. **d-f**, Endogenous Rab11 expression at the apical surface. **d**, in WT discs, Rab11 presents as small grainy particles. **e**, Rab11 expression is greatly diminished by EF, **f**, but not LF. **g-l**, DEcad expression at the apical surface, at the AJ. **g**, in WT discs. **h**, EF, and **i**, Rab11 DN decreases levels and disrupts patterns of AJ. **j**, Sec15-GFP forms vesicles which are decreased in levels by: **k**, EF; **l**, Rab11(DN); and **n**, LF. **m**, Rab11(WT) rescues Sec15-GFP vesicles from EF, and **o**, has a small rescuing effect of Sec15-GFP vesicles from LF.

reduced or not reduced at all, suggesting EF does not lead to general loss of integrity of the AJ.

Effects on Sec 15, which colocalizes with Rab11 to form the exocyst complex, was also investigated by Annabel Guichard and Beatriz Cruz-Moreno. Sec15-GFP in imaginal discs forms large Sec15 vesicles and a diffuse cytoplasmic staining (Fig. 3j). EF was found to indirectly diminish sec15 vesicles and weakened colocalization with Rab11 (Fig. 3k). Rab11(DN), behaved similarly to EF by diminishing Sec15 vesicles (Fig. 3i). Complimenting that data, the effects of EF on Sec15 vesicles were rescued by expression with Rab11(WT) (Fig. 3m). This demonstrated EF reduced Sec15 vesicles through its effects on its partner Rab11.

LF also diminished Sec15 vesicles and weakened colocalization with Rab11 (Fig. 3n). However, LF did not show a significant effect on Rab11 levels and its effect on Sec15 staining was only weakly rescued by Rab11, indicating LF does not inhibit Sec15 through Rab11 (Fig. 3f,n,o). Interestingly, inhibition of Sec15 was linked to Notch-like phenotypes. An explanation to previous studies indicating synergism between LF and EF was finally given^{50,51}: they synergize by affecting two interacting components of the exocyst.

A few of the other Rab crosses produced notable phenotypes as well. As an example, Rab35 (DN) produced elongated wings with a shallow bowl-like curve and thickened L3 vein. It would be interesting to see if Rab35 (DN) synergizes with LF. Interesting to note, Rab35 is located on the recycling

endosome⁶⁰. A summary of all Rab results can be viewed in supplementary Table 1.

Decreasing expression of Sec15, Sec5, and Exo70 strengthens the LF phenotype

The Rab screen proved to be effective in identifying Rab11 as a mediator of EF activity, which led to the identification of the exocyst component and Rab11-binding partner Sec15 as a target of LF^{17,62}. A second screen was then initiated, to determine whether known exocyst components and regulators were involved in the cellular response to EF and LF toxins. This screen made use of available RNAi lines, including a variety of different genes with the potential in being involved with the toxins' pathway. The screen included genes of core exocyst components and its regulators, mediators of vesicle fusion, junctional proteins, cAMP effectors, Rab11-adjacent genes, and others.

As noted earlier, Sec15 was found to be inhibited by LF¹⁷, so other core components of the exocyst were tested in this RNAi screen to see if they too would have a role in the response to LF intoxication. The core exocyst components tested were: Sec3, Sec5, Sec6, Sec15, Exo70, and Exo84. Sec8 and Sec10 were not tested, simply because we did not have the RNAi lines for those components at the time. All tested Sec components except for Exo70 produced a strong phenotype when knocked out by RNAi (Fig. 4), indicating the importance of the core exocyst for proper wing development. The severity of the Sec RNAi phenotypes made comparing the effects of the RNAi to the effects of

coexpressing the RNAi with either toxin, more difficult. I focused on the effects of the RNAi lines for Sec15, Sec5, and Exo70, because they were the most clear.

Strong wing-specific expression of Sec15 RNAi (Sec15^{RNAi}) produced a very severe wing phenotype in which the wings were severely reduced in size and shriveled up. The phenotypes were too severe to be compared to one another, so the crosses were repeated at 18°C, where the expression of the RNAi would be weaker. Although still producing severe phenotypes, the severity was reduced, and it could be seen that Sec15^{RNAi} coexpressed with LF had a more severe phenotype than with Sec15^{RNAi} alone or with Sec15^{RNAi}+EF (Fig 4a,b & Sup. Table 2). This is consistent with previous data pointing to LF's inhibition of Sec15 activity¹⁷, and serves as a case in point that the RNAi screen can be used to identify other targets of the LF or EF pathway.

Reducing Sec5 levels also showed an enhancing effect with LF (Fig. 4c-f). Two different Sec5 RNAi lines were used. The first Sec5 RNAi (Sec5^{RNAi}) used increased the intensity of the LF phenotype despite showing only a mild size reduction when expressed alone (Fig. 4c,d). The other Sec5 RNAi line, Sec5 RNAi-Trip (Sec5^{RNAi-TRIP}), produced a severe phenotype when expressed alone, but produced an even more severe phenotype with LF (Fig. 4e,f). The differences between the intensities of the two RNAi lines are likely to be due to differences in expression levels. Despite this variability in phenotype intensity of different RNAi lines, a consistent message was delivered: reducing Sec5 enhances the LF phenotype.

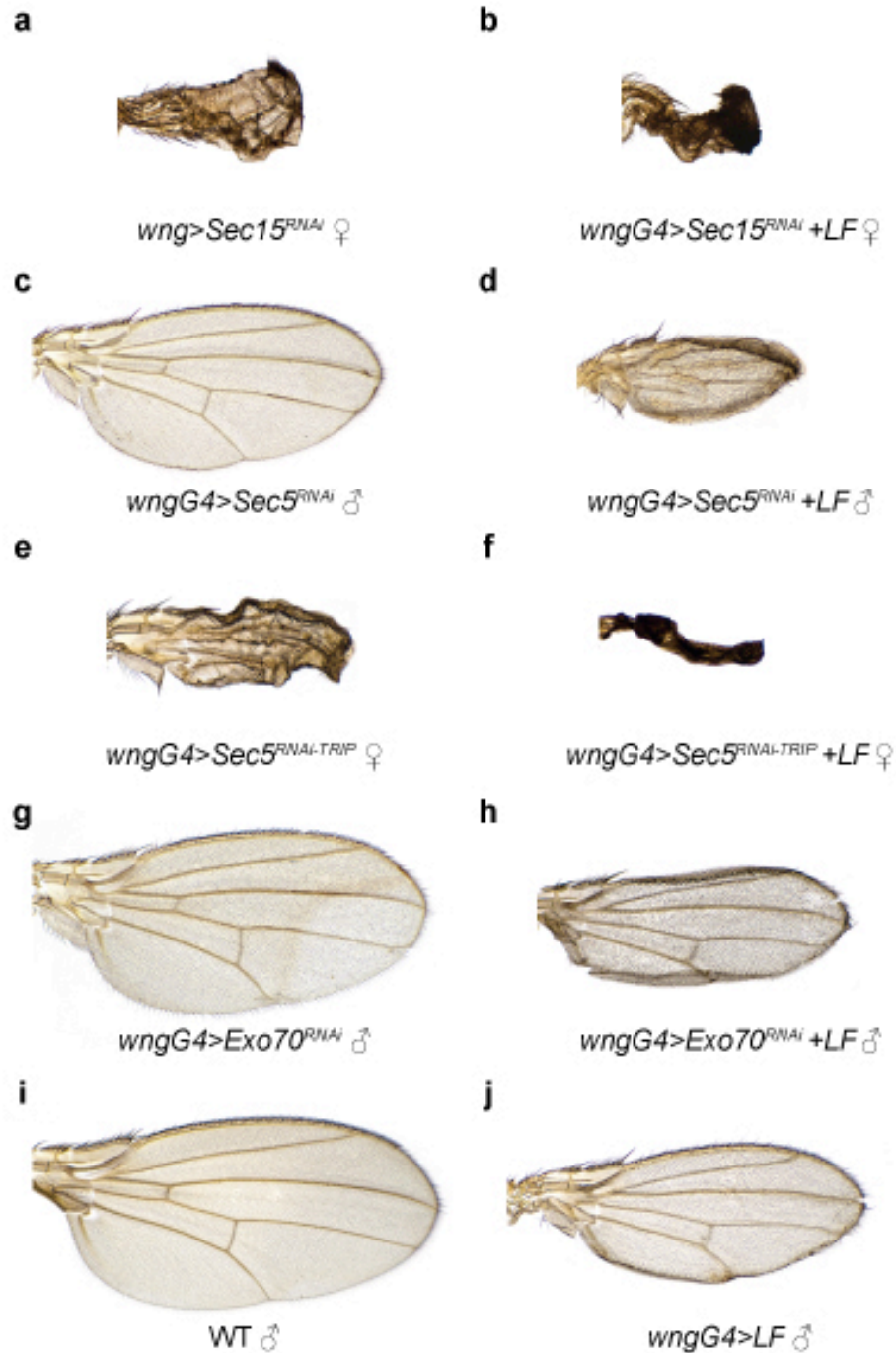


Figure 4: Decreasing expression of Sec15, Sec5, and Exo70 strengthens the LF phenotype. Wing phenotypes for the following genotypes: **a**, *wngGAL4>Sec15^{RNAi}*; **b**, *wngGAL4>Sec15^{RNAi}+LF3x*; **c**, *wngGAL4>Sec5^{RNAi}*; **d**, *wngGAL4>Sec5^{RNAi}+LF3x*; **e**, *wngGAL4>Sec5^{RNAi-TRIP}*; **f**, *wngGAL4>Sec5^{RNAi-TRIP}+LF3x*; **g**, *wngGAL4>Exo70^{RNAi}*; **h**, *wngGAL4>Exo70^{RNAi}+LF3x*; **i**, WT; **j**, *wngGAL4>LF3x*; **i**, is included as a reference for comparison for **g**, Exo70^{RNAi} and **h**, Sec5^{RNAi} wings and **j**, is included as a reference for comparison of **h**, Exo70^{RNAi}+LF and **d**, Sec5^{RNAi}+LF wings

Similarly, coexpression of Exo70 RNAi (Exo70^{RNAi}) with LF showed an enhancement of the LF phenotype as well, but not as strongly as Sec5^{RNAi}+LF (Fig. 4c-h). Expression of Exo70^{RNAi} alone produced a very slight wing curvature, which can only be seen in males. This may be because the loss of Exo70 does not effect exocytosis as drastically as the loss of any of the other exocyst components, or it may be a weak RNAi line.

Decreased levels of CG5745 and CG17282 disrupt exocyst function in similar fashion

Rab11 and Sec15, targets for EF and LF, respectively, are functional and binding partners⁶². Interestingly, the genes that encode them are also located near each other in the genome, separated by only one gene⁶³. This suggested that other exocyst partners might be located in this genomic segment, and possibly be affected by the toxins as well. It turned out, six out of the seven Rab11 adjacent genes produced wing phenotypes when expression of that gene was reduced via RNAi. (Fig. 5 and Sup. Table2). Of these, I restricted my subsequent analysis to CG5745^{RNAi} and CG17282^{RNAi}, which seemed the most promising.

CG5745 contains a GTPase Activating Protein specific for Rab (Rab-GAP) domain⁶⁴. Expressing CG5745^{RNAi} produced two different phenotypes. The predominating, milder phenotype consists of smaller, curved wings and thickened veins. The second, stronger phenotype, appears as “blisters” similar to ones

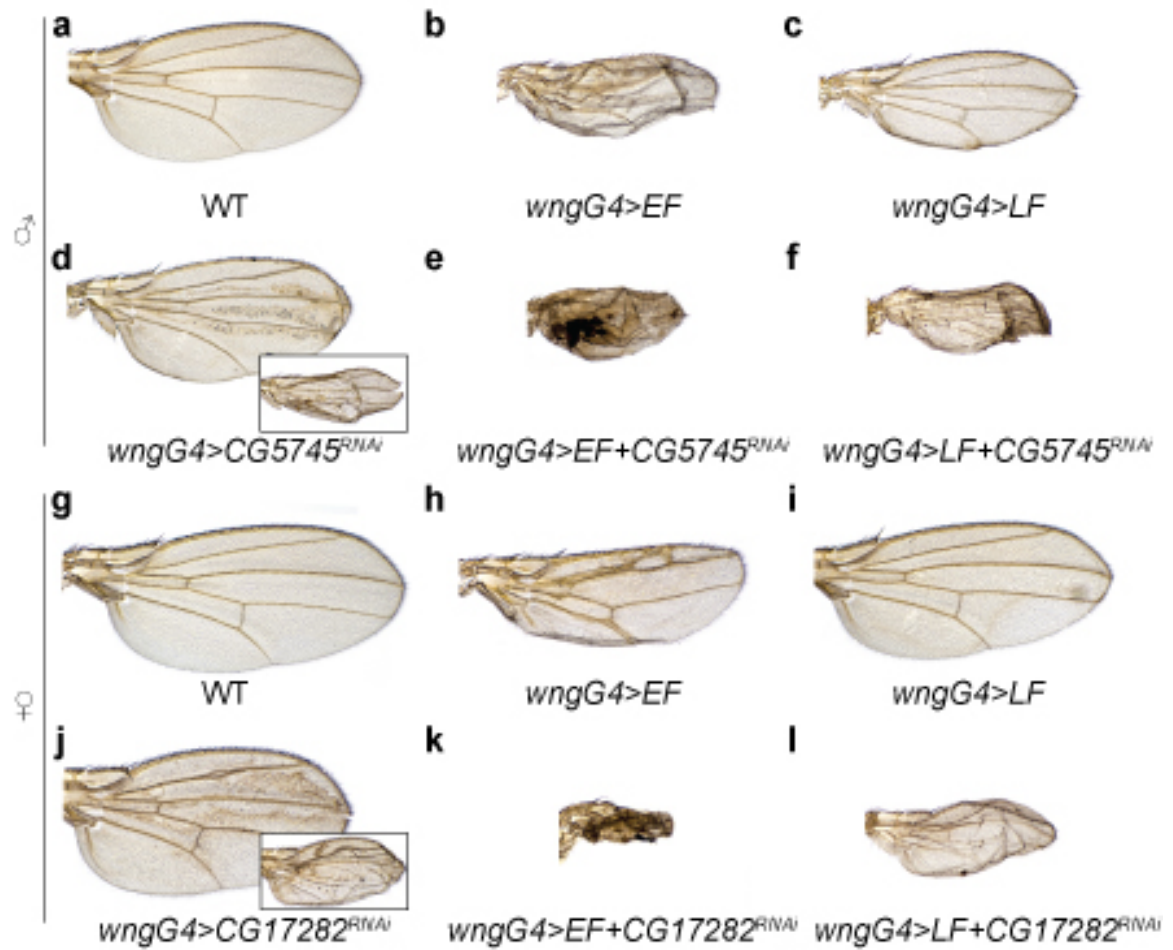


Figure 5: CG5745^{RNAi} and CG17282^{RNAi} increase the strength of the EF and LF phenotype. Wings of the following genotype: **a, g**, WT; **b, h**, *wngGAL4>EF*; **c, i**, *wngGAL4>LF3x*; **d**, *wngGAL4>CG5745^{RNAi}*; **e**, *wngGAL4>EF+CG5745^{RNAi}*; **f**, *wngGAL4>LF+CG5745^{RNAi}*; **j**, *wngGAL4>CG17282^{RNAi}*; **k**, *wngGAL4>EF+CG17282^{RNAi}*; **l**, *wngGAL4>LF+CG17282^{RNAi}*. Male flies express wing phenotypes more strongly than females, so **a-c**, serve as references for comparison for **d-f**, and **g-i** serve as references for comparison for **j-l**. **d,j**, Insets show the secondary phenotype presented in **d**, CG5745^{RNAi} and CG17282^{RNAi} wings.

seen in EF (Fig. 5d). When coexpressed with dicer (Dcr), an enzyme involved in the RNAi pathway⁶⁵, this phenotype became even stronger, as would be expected from a partial inhibition of gene activity by CG5745^{RNAi} expressed alone. Coexpression with EF resulted in a stronger phenotype in general, but it is unclear if this is due to an additive or synergistic effect. (Fig. 5e, b). Coexpression with LF, resulted in smaller wings commonly characterized with a “blister” (Fig. 5).

As CG5745 is a predicted RabGAP⁶⁴, it could be a negative regulator of Rab11. Considering this, and the wing phenotypes resulting from expressing CG5745^{RNAi} and coexpression of CG5745^{RNAi} with EF or LF, I decided to investigate if reduction of CG5745 expression leads to defects in exocyst function, similar to EF and LF. CG5745^{RNAi}, when expressed with Sec15GFP, caused a significant reduction in the number of Sec15GFP vesicles in the wing disc. Remaining vesicles are smaller and some show irregularity in shape (Fig. 6a, b). Interestingly, Rab11 levels increased drastically (Fig. 6d, e). Rab11 colocalization with the remaining Sec15GFP was not disrupted, as occurs with EF.

This disruption in the levels of Sec15 and Rab11 led me to further investigate effects on the exocytosis, so I checked if trafficking of DECad and Delta to the AJ was disrupted. DECad and Delta are known membrane proteins whose trafficking to the AJs depends on endocytic recycling^{66,67}. DECad at the apical level of the wing disc normally shows ubiquitous expression, with a pattern showing an accumulation at the primordial veins and developing wing margins

(Fig. 6g). Decreasing CG5745 via RNAi reduced overall levels of DECad and caused a disruption in its expression pattern. There was a nearly complete loss of high expression in the primordial veins and the margin on the dorsal side (Fig. 6h). Preliminary results with Delta, which is restricted to the veins and margins as well, also shows an overall reduction and a nearly complete loss of vein and margin expression on the dorsal side (data not shown).

The function of CG17282^{RNAi} is unknown, but considering its phenotypic effects I decided to look into it further. A pBLAST search of the protein sequence brought up peptidyl-prolyl isomerases as the most common match. CG17282^{RNAi} produced a “mild” wing phenotype and minority “blistering” phenotype, similar to CG5745^{RNAi} (Fig. 5j). Coexpression with EF shows a consistently severe phenotype, significantly stronger than would be expected if the effect was additive (Fig 5k). CG17282^{RNAi}+LF wings commonly presented with a blister, and were much smaller than both LF and CG17282^{RNAi} expressed alone, suggesting synergy with LF as well (Fig. 5l).

CG17282^{RNAi} showed effects on Sec15 vesicles very similar to that of CG5745^{RNAi}: reduction in number and size of Sec15GFP vesicles and some irregularity in vesicle shape (Fig. 6a, c). Initial results show an increase in Rab11 levels as well as weakening of the colocalization between Sec15 and Rab11 (Fig. 6f, i). If this reduced colocalization is verified with repeated experiments, it would be of interest, as EF weakens colocalization between Rab11 and Sec15 as well¹⁷.

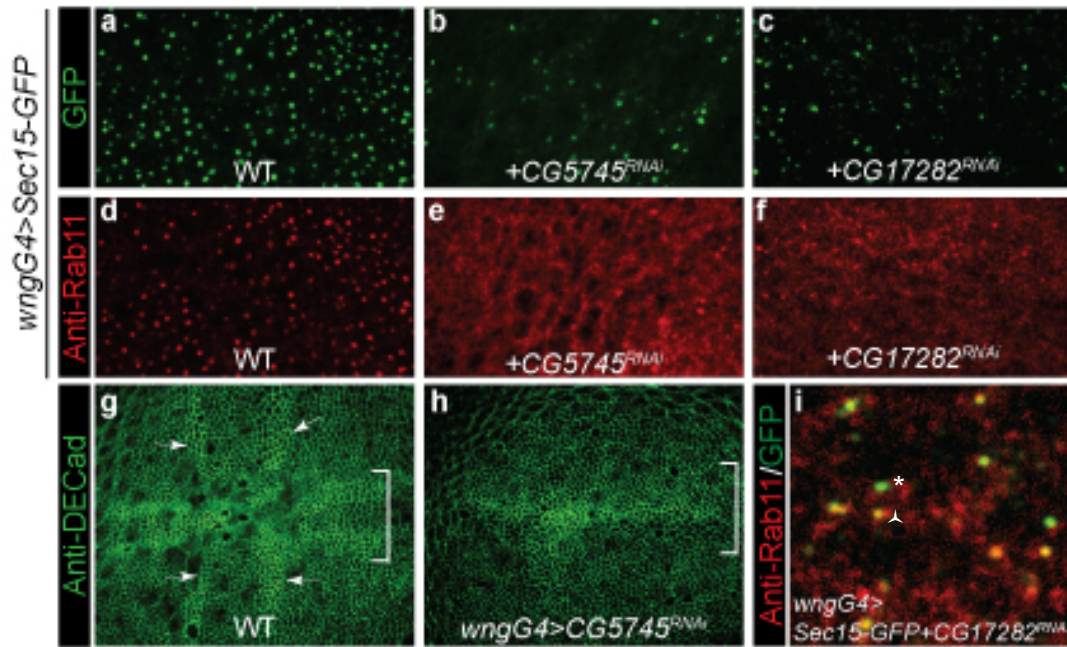


Figure 6: Loss of CG5745 and CG17282 disrupt levels of exocyst partners Sec15 and Rab11 in a similar fashion. **a**, Sec15-GFP vesicles in WT discs. **b**, When Sec15-GFP is coexpressed with CG5745^{RNAi} and **c**, CG17282^{RNAi}, levels of Sec15 vesicles decrease, and remaining vesicles are smaller and show irregularity of shape. **d**, Rab11 levels in WT discs. **e**, CG5745^{RNAi} and **f**, CG17282^{RNAi}, show an increase in Rab11 levels. **g**, DECad stain in WT disc shows DECad at points of cell-to-cell junction, and a pattern in which DECad accumulates at the primordial margin (brackets) and primordial wing veins (arrows). **h**, Primordial margin on dorsal side disappears in CG5745^{RNAi}-expressing wings. **i**, Sec15-GFP+CG17282^{RNAi} showing delocalization of Sec15 and Rab11. * shows an example of delocalization, whereas ^ points out a Sec15 vesicle that still colocalizes with Rab11

Discussion

The purpose of both the Rab and RNAi screen was to identify potential novel targets for anthrax toxin activity. None of the results are meant to provide definitive answers, but serve as a guide as to which proteins should be further studied as candidates for mediating toxin activity.

In the Rab screen I conducted, only one dominant negative (DN) mutant showed a phenotype nearly identical to EF: Rab11(DN). The Rab11 GTPase is critical for endocytic recycling, a process in which some membrane-bound proteins can be redirected at the cell surface after endocytosis⁶⁰. In addition, Rab11(WT), which caused no phenotype on its own, weakened the EF phenotype when coexpressed. Taken together, the data suggested EF inhibited Rab11, which would explain why inhibiting Rab11 via DN caused a similar phenotype and why increasing the dose of Rab11 with Rab11(WT) rescued the wing. This provided high promise as Rab11 being a target for EF. These findings led to further experiments by my colleagues confirming EF inhibits Rab11, which then led to identifying Rab11's binding partner Sec15 as a target of LF activity¹⁷. Not only were new targets found, but this provided a cellular mechanism behind the synergistic, physiological effects found by previous studies^{17,50,51}.

Only few other Rabs showed effects as a DN or WT, suggesting that they have no function in the wing, or that they have redundant functions (Sup. Table1). None were as promising as Rab11, but a couple others might be worth looking into, such as Rab35. Rab35, like Rab11, regulates the recycling

endosome⁶⁰. Expressing Rab35(DN) in the wing produced somewhat elongated, curved wings with thickened veins, reminiscent of the LF phenotype. Rab35(WT) produced no phenotype on its own, and had no effect on EF, but it would be interesting to test if it has the ability to rescue the LF wing phenotype, as well as to see if Rab35(DN) synergizes with LF/EF. It would also be of interest to see if Rab11 and Rab35 co-localize, and if Rab11 expression can rescue Rab35(DN) phenotype, and inversely, if Rab35(WT) can rescue the phenotype of Rab11(DN).

Previous results showing Sec15's role in LF activity¹⁷ prompted the investigation of the other core exocyst components. Five out of the six exocyst components produced severe phenotypes, which made it more difficult to interpret their interactions with EF and LF. The results for Sec5^{RNAi}, Sec5^{RNAi-TRIP}, Sec15^{RNAi}, and Exo70^{RNAi} were clearer than the others and consistent with expectations. When each of these RNAi lines was coexpressed with LF, an enhanced phenotype was seen (Fig. 4), pointing to these sec components as candidates for LF activity. As noted above, Sec15 had already been independently verified as being inhibited by LF, providing, as Rab11 did, an example of the usefulness of genetic screens as a starting point for the identification of toxin targets.

Results from the two different Sec5 RNAi lines show a phenotype enhancement of LF, suggesting a relationship between Sec5 and the LF pathway. This may indicate an inhibition of Sec5 by LF activity. Another possibility is that the phenotype enhancement is caused by a more indirect effect,

that disrupting Sec5 exaggerates LF's targeting of Sec15 by further disrupting the core exocyst. It has been found that loss of function *Sec5⁻* and *Sec15⁻* behave similarly in disrupting the targeting of DECad to the AJ, accumulating instead, in enlarged Rab11 recycling endosomal compartment⁶⁶.

Further experiments need to be carried out to determine the relationship between Sec5, Sec15, and LF. An appropriate follow-up experiment would be to see if endogenous Sec5 or Sec5GFP levels in the wing disc are affected by LF. Another informative experiment would be to see if Sec15 vesicles can be rescued by Sec5(WT). Rescuing vesicles would indicate LF effects are mediated, in part, by its actions on Sec5.

LF is a zinc metalloprotease that cleaves MAPKKs, and it has been confirmed its activity extends to the known *Drosophila* MAPKKs Dsor, Licorne (Lic), and Hemipterous (Hep)^{44,57}. Thus, I would coexpress Sec5^{RNAi} with each of the *Drosophila* MAPKK RNAi lines to see if there is a synergy of wing phenotype. The Dsor^{RNAi}, Lic^{RNAi}, Hep^{RNAi}, and MKK4^{RNAi} lines can also be used to see if they lower levels of Sec5GFP as well.

A LF phenotype enhancement is also seen in Exo70^{RNAi}+LF wings. The same questions that came up with the synergy seen by Sec5^{RNAi} needs to be addressed here as well. It has been shown that extracellular signal-regulated kinases 1/2 (ERK1/2), phosphorylate Exo70, which enhances the binding of Exo70 to other exocyst components and helps regulate its assembly⁶⁸. ERK1/2, in turn, has been shown to be activated by the MAPKK MEK1 (human homolog of Dsor)^{57,69}. Considering Dsor, along with the other MAPKKs, are cleaved by LF,

it is very likely LF inhibits normal functioning of Exo70 by disrupting the Dsor/ERK(1/2)/Exo70 pathway. Follow-up experiments proposed for Sec5 can also be utilized for verifying LF's inhibition on Exo70.

Thickened veins, wing curvature, and EF-like blisters characterize the CG5745^{RNAi} wing phenotype. When coexpressed with EF or LF, enhanced phenotypes result (Fig. 5a-f). The increased strength of the EF phenotype in CG5745^{RNAi}+EF wings resulted in a stronger phenotype in general, but the enhancement was not consistent, and it is unclear if the increased strength is due to a synergistic effect or an additive one. When expressed with LF, the wings were smaller and caused a "blister" (Fig. 5f). This "blistering" effect showed to be a predominant feature of the wings, indicating the effect is not merely an additive effect, but likely a synergistic one.

Reducing CG5745 via RNAi caused a disruption of DEcad and Delta expression at the adherens junction, as well as diminished Sec15GFP vesicles at the apical surface (Fig. 6). These are all similar to effects caused by EF and LF. The upregulation of CG5745^{RNAi} on Rab11, however, conflicts with the downregulating effects of EF on Rab11. It would be interesting to know what about the loss of CG5745 causes these similar effects with EF and LF, and how it differs to produce the opposite effect on Rab11 levels.

CG5745 has not been well studied. Blast results show CG5745 is part of the Rab/GAP-TBC super-family⁶⁴. A survey of databases found CG5745 has two closely related human homologs, FLJ20322 and C22ORF4⁷⁰, implying conserved activity. It is not known which Rabs CG5745 is specific too. It is expected that in

the CG5745^{RNAi}-expressing discs, Rabs affected by CG5745 would remain in their active form. Rabs can be activated through a Rab guanine nucleotide exchange (GEF) cascade⁷¹, so Rabs downstream of CG5745's substrate may also be activated in higher numbers than usual. However, the existence of a countering Rab-GAP cascade, in which the newly activated Rab recruits the GAP, of the preceding Rab, may prevent the over-activation of downstream Rabs⁷²

My data, which shows an increased expression of Rab11, suggests some sort of relationship between CG5745 and Rab11 (Fig. 6e). It would be of interest to know if CG5745 is specific for Rab11, or for another Rab which act upstream of Rab11. Determining this would require more research. The transgenic *UAS-Rab* lines used in the EF screen, can be used in a screen with CG5745^{RNAi}, as well as CG5745(WT), to see if there are interactions with other Rabs and CG5745. The increase of Rab11 levels could be quantified by Western blotting and the ratio of GTP-bound to GDP-bound Rab11 could be determined by immunoprecipitation experiments of Rab11 with its partner Sec15. *In situ* experiments would show if the increased Rab11 seen in the CG5745^{RNAi}+Sec15, is due to an increased production of Rab11, or a decreased degradation.

CG17282^{RNAi} behaved with incredible similarity to CG5745^{RNAi}. CG17282^{RNAi} had a similar wing phenotype to CG5745^{RNAi}. Enhanced expression with EF, however, was a much stronger one that more clearly indicated synergy. Effects on Sec15 and Rab11 expression are also similar to CG5745^{RNAi}. The function of CG17282 has not been established. In a pBLAST search⁶⁴, most

matches were to peptidyl-prolyl isomerases, which facilitate the *cis-trans* isomeration of peptide bonds within polypeptide chains. If CG17282 is indeed an isomerase, it may be its substrate is a mediator of EF and/or LF activity, explaining the synergy indicated by CG17282^{RNAi}+EF and CG17282^{RNAi}+LF wings. It can be that as an isomerase, it is a regulator for a component of the Rab11/Sec15 pathway. CG17282^{RNAi} was picked because of its proximity to *Rab11* and *Sec15* on the genome after all, with the idea that *Rab11/Sec15* adjacent genes might be part of a functionally related “gene cluster.”

Significance of the RNAi screen beyond anthrax

The purpose of this screen was to identify mediators of anthrax toxin activity, but this screen can be used as a starting point for other experiments as well, such as *Drosophila* wing development or for the study of “gene clusters” in *Drosophila*.

Since Rab11 and Sec15 are known partners, and their genes are located in close proximity to each other, adjacent genes *Slmb*, *Peter Pan (Ppan)*, *Rtet*, *rhoGAP93B*, *CG17282*, *CG5745*, and *CG7044*, were included in the RNAi screen, with the idea that other partners might be located in this region as a gene cluster. The similarities seen between CG5745 and CG17282 are in concert with this idea. However, I followed up on only two of the seven Sec15/Rab11 adjacent genes, but six out of the seven RNAi lines produced phenotypes. *Ppan*^{RNAi}, *rtet*^{RNAi}, and *RhoGAP93B*^{RNAi}, also showed stronger EF and/or LF phenotypes, though further investigation is needed to verify if the enhanced phenotype is

additive or not. In addition, *Ppan*^{RNAi}, expressed with VgGal4, a wing GAL4 which drives expression in the wing margin, produced wing notches remarkably similar to those produced by Notch mutants and EF¹⁷ (Sup. Table2). As more genomes are getting sequenced, the previously held thought that eukaryotic genes are ordered at random is being challenged⁷³. It may be that this region composes a “gene cluster” in *Drosophila*, and add more weight to this newly developing paradigm.

II

The generation and analysis of dominant negative mutants of Lethal Factor

Results

Construction and characterization of *UAS-LF_T* and *UAS-EF_T* transgenes

Individuals infected with anthrax present with flu-like symptoms at the onset of the second, fulminant stage. By this point of infection, bacterial toxins have reached such high titers that death usually results even with effective antibiotic treatment. For this response, there is a need to develop therapies targeting EF and LF. For my second project, I used *Drosophila* and the toxin-induced wing phenotypes to screen for dominant-negative (DN) versions of EF and LF by mutagenesis.

I developed DNA constructs for tagged versions of LF and EF (LF_T and EF_T, respectively) to be used to generate transgenic UAS-LF_T and UAS-EF_T *Drosophila*. The purpose of this was to add more options for the analysis of LF and EF mutants I planned to generate (such as Western Blotting, or immunofluorescence). Doing PCR with primers I designed, I generated a LF_T sequence containing one copy of the epitope tag FLAG and HA in the N terminus and C terminus, respectively (Fig. 7a). The EF_T sequence was built with HSV in the N terminus and c-Myc in the C terminus (Fig. 7b).

LF_T and EF_T genes were inserted into fly embryos with a *white*⁻ background, to allow easy selection of transformants carrying the *white*⁺ marker placed after the gene of interest in the transgenic construct. Like many other transgenes introduced into *Drosophila*, they are derived from a P element, a type

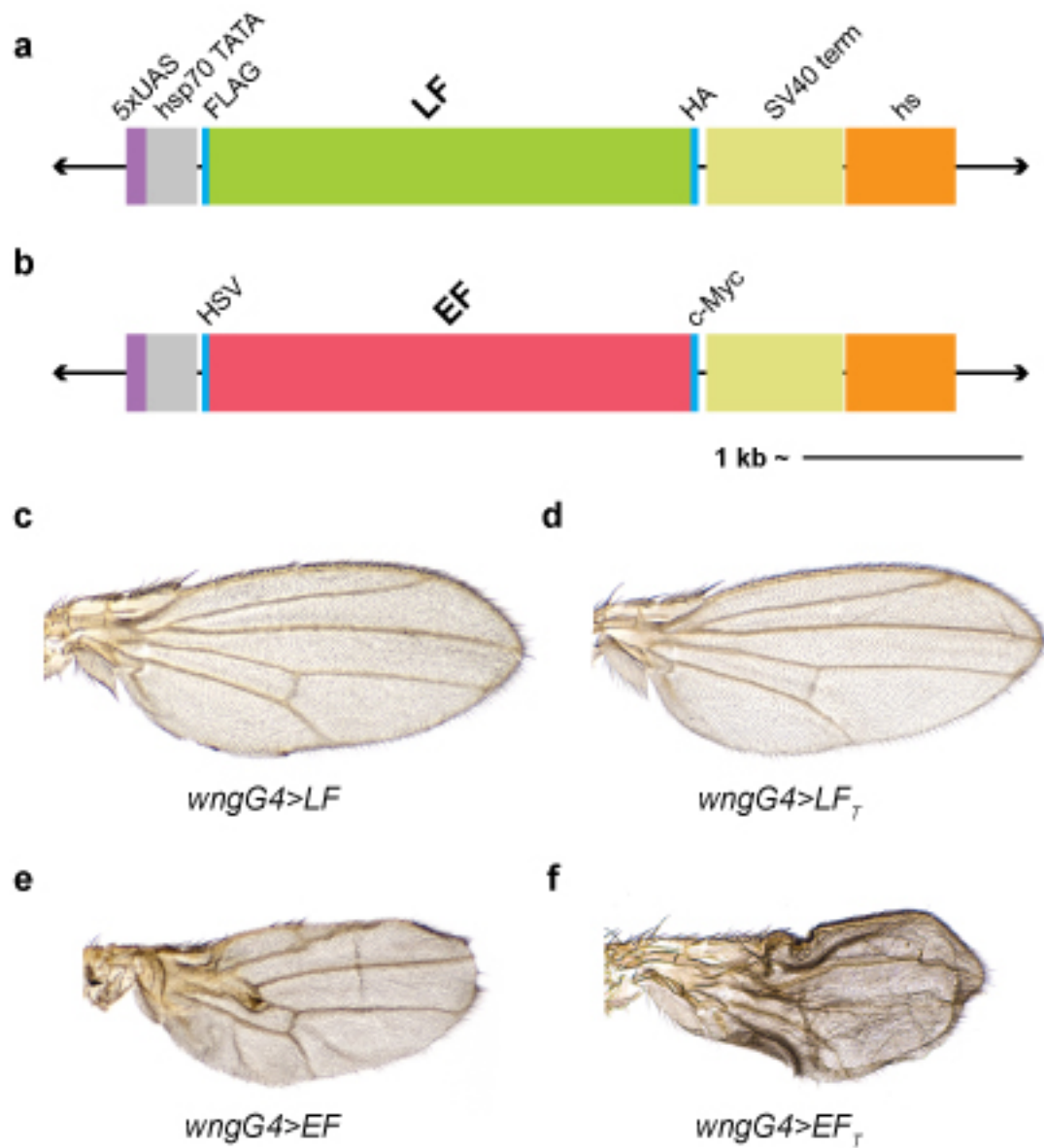


Figure 7: Lf and Ef transgenic fly lines. **a,b**, DNA constructs of **a**, Lf tagged with FLAG and HA and **b**, Ef tagged with HSV and c-MYC (epitope tags not drawn to scale). **c-f**, Wings of the following genotypes: **c**, *wngG4>LF* (refers to *wngG4>LFG2x*), and *wngG4>Lf*. **e**, *wngG4>EF*

of transposon specific to *Drosophila*, but lack the sequences necessary for transposition⁷⁴.

LF_T expressed with wngGAL4 causes a phenotype similar to a previously characterized LF stock⁵⁷: small, scooped wings elongated along the proximal-distal axis (compare Fig. 7d to 7c). EF_T, when expressed with wngGAL4, results in slightly shriveled, small wings with increased hair growth and L2 and L3 veins that are closer together (Fig. 7f). This stock is less variable and stronger than the previously established *UAS-EF* stock⁵⁷ (compare Fig. 7f to e). Phenotypic differences between the two stocks could occur as they are different inserts, which may lead to different expression levels or dynamics. In addition, the untagged *UAS-EF* contains an excisable FRTwhiteFRT cassette whereas *UAS-EF_T* does not.

Detection of LF_T by Western blotting, using antibodies against FLAG and HA was successful, but I was unable to visualize EF_T through Western blotting. Staining for LF_T and EF_T in the wing imaginal disc, using respective antibodies against their immunological tags was also unsuccessful, despite attempting different fixation methods and different antibody concentrations.

Δ2,3 screen identifies two dominant negative versions of LF_T

Δ2,3 transposase was used as a mutagen on LF_T and EF_T genes, with the goal of generating a dominant negative which could be developed into an anti-toxin drug, fit for human use. After excision by Δ2,3 transposase, gap repair occasionally results in rearrangements such as deletions, duplications, and

inversions⁷⁵. Potentially-mutated LF_T (ΔLF_T) and EF_T (ΔEF_T) were crossed with flies carrying their respective WT counterparts, expressed at high levels in the wings. The F1 progeny were screened for flies showing a weakened phenotype (Fig. 8a). Dominant negative (DN) candidates were found for both, but only LF DN candidates showed a confirmed DN activity.

Two of the isolated candidates for LF dominant negatives survived and led to established stocks with confirmed DN activity. Coexpressing each of the two candidates with LF(WT) using *wngGAL4* showed suppression of the LF wing phenotype (compare Fig. 8d-e to c). In both cases, the LF phenotype is not completely suppressed, but partial suppression is 100% penetrant, with LF_T DN2 having the stronger suppressing effect. LF-induced wing curvature, which is more apparent in females, was completely or almost completely flattened in all that had either LFTDN (Fig. 8a-d, top panel). Males also showed flatter wings and slight to moderate size recovery (Fig. 8a-d, bottom panel). To verify my visual observation of suppression with quantifiable data, I measured the lengths of male wings and found LF_T DN1 had a 22.5% rescue in length and LF_T DN2 had a 41% rescue in length. A T-test found the likelihood of the rescued length being due to chance as $5.76077E-07$ for LF_T DN1 and $7.68574E-6$ for LF_T DN2, both significantly low enough to reject the null hypothesis. The wing length recovery is only one aspect of recovery. The thickness of wing veins becomes more normal, and the effect on curvature, which shows a near-complete suppression, is harder to quantify. Neither LF_T DNs had an inhibiting effect on the EF wing phenotype (data not shown).

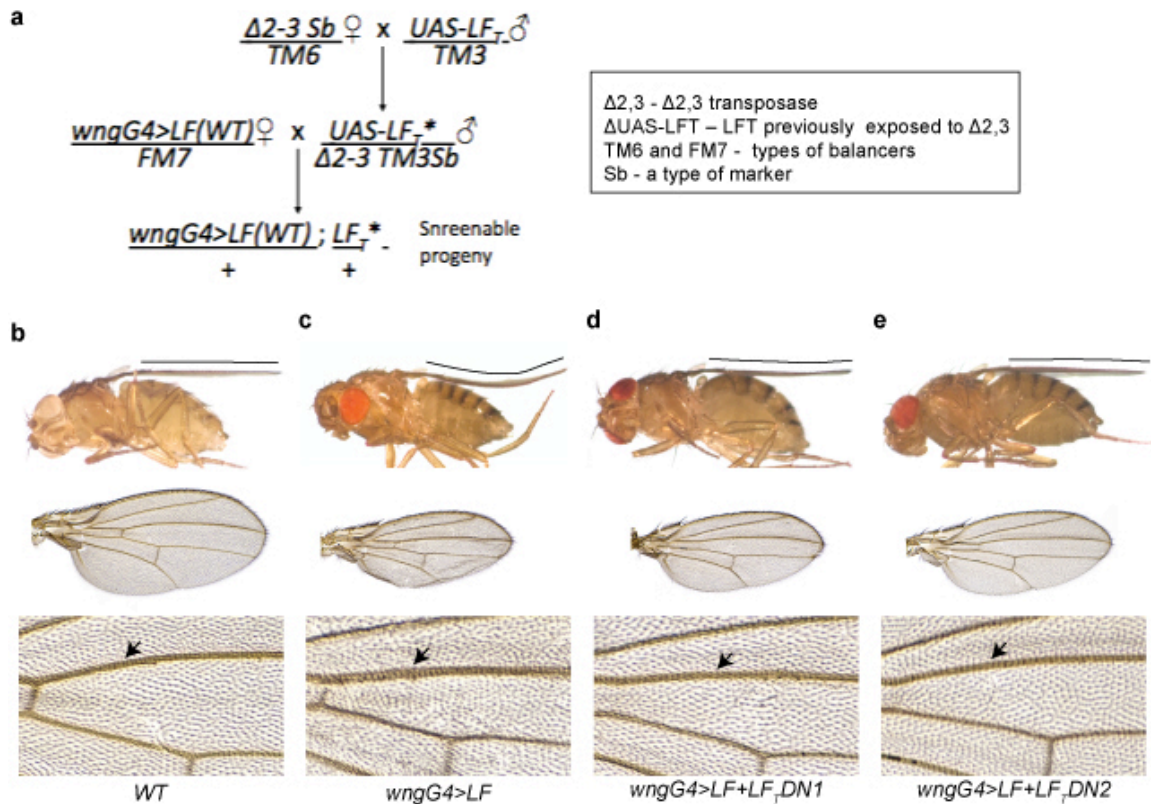


Figure 8: Δ2,3 screen generates two dominant negatives against LF. **a**, Cross scheme of Δ2,3 screen with LF_TDN . Δ2,3 stands for Δ2,3 transposase. ΔUAS- LF_T refers to LF_T which has been previously exposed to Δ2,3. TM6 and FM7 are balancers. Sb is a marker. **b-e**, Wings for the following genotypes: **b**, WT; **c**, wngG4>LF_T ; **d**, $\text{wngG4>LF}_T+\text{LF}_T\text{DN1}$; **e**, $\text{wngG4>LF}_T+\text{LF}_T\text{DN2}$. Wings in the upper panel show the curve phenotype, which is especially apparent in females. The line drawn above each wing represents the curve along the wing margin. Middle and lower panels show wings from male flies, which demonstrate the change in size, shape, and vein thickening. Arrows in bottom panel point out areas of thickened vein, which decreases with both LF_TDN s

I proceeded in my next steps of analyzing these LF-DN with the assumption that both mutants had intact UAS sequence and 5'-most regions of the LF gene, since mutations in the UAS sequences would prevent their Gal4-dependent expression. In my first attempts at PCR, I used four different antisense (AS) primers, all past the LF_T sequence. Two of these AS primers bind within the SV40 polyadenylation sequence and the other two in the *white+* region. None of these produced detectable PCR products from the mutant DNA, suggesting that the lesions affected more 5' regions. I then moved on to a "staggered PCR" method, for which I used AS primers starting from the 3' end of LF_T moving towards the 5' regions of the LF_T sequence (Fig. 9a). An AS primer producing the right PCR product would show that part of the DNA sequence was still intact, thus narrowing down the area of the "breakpoint," where the end of the mutant sequence would be. LF_TDN1 showed the breakpoint is before the 809th base-pair (Fig. 9b). LF_TDN2 has its breakpoint past the 782nd base pair but before the 2,146th base pair (Fig 9c). These results not only narrowed down the sequence breakpoint in my DNs, but it also verified my assumption that the mutation did not occur at the 5' end.

Western blotting using anti-FLAG and anti-HA did not detect either LF_TDN. If the mutation resulted in a protein-encoding gene, the lack of detection by anti-HA would be expected, as the C-termini end of both LF DNs would be missing. However, the FLAG tag should still be intact. The LF_T control was detected, indicating the antibodies and the Western blotting protocol was working. Since it is possible that my DN mutants have RNAi activity (as it has been previously

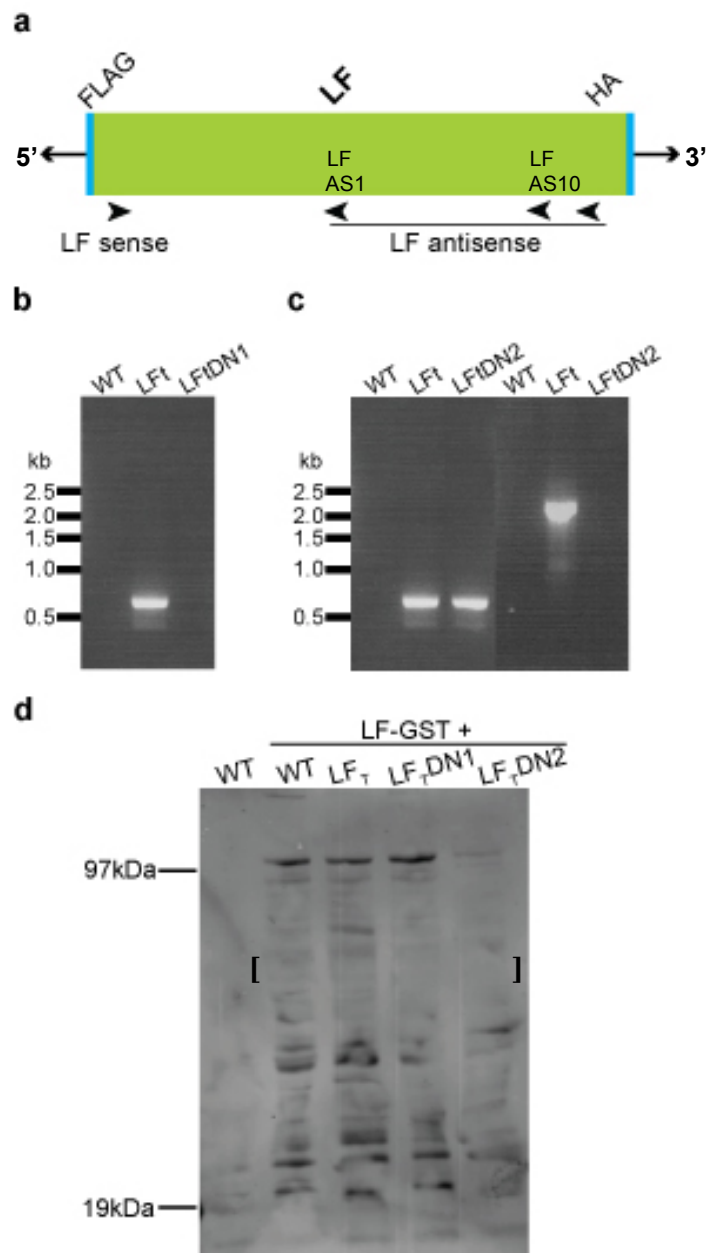


Figure 9: Analysis of LF DN activity. **a**, represents a scheme for staggered PCR method using antisense primers starting from the 3' end, and moving towards the 5' end of the LF_T sequence. LFAS4 antisense primer anneals between the 783rd and 809th base pairs on the LF sequence. LFAS10 antisense primer anneals between the 2,119th and 2,146th base pairs on the LF sequence, **b**, PCR reaction showing LF4 antisense does not produce a product for LF_TDN1, indicating mutation occurred before the 809th base pair. **c**, shows LF4 antisense forms a product for LF_TDN2, indicating LF_TDN2 sequence contains at least the first 809 base pairs of LF_T. LF10 antisense, which goes up to 2,146 base pairs, does not produce a LF_TDN2 product. **d**, LF-GST band indicated by brackets. LF_TDN2 decreases LF-GST expression, almost completely

shown with this method⁷⁶), which would explain why a product was not detected with Western blotting. I followed up with an experiment to see how the two LF DN_s affected LF levels and found that LF_TDN2 decreased LF expression drastically, suggesting this mutant exerts its inhibition through RNAi. LF_TDN1, however, did not decrease LF levels.

Δ2,3 transposase is effective at causing mutations on UAS-EF_T

A Δ2,3 screen for EF_T was also conducted. Although 12 candidates survived and produce progeny, subsequent tests showed that none of them had dominant negative activity, in stark contrast to LF which had two surviving candidates, both of which proved to be true DN. Aside from the screenable progeny (wngGAL4>EF+ΔEF_T), the cross produced flies with the genotype wngGAL4>EF_T. EF_T normally has a strong phenotype (Fig. 7f), but amongst this progeny, I saw flies with barely any phenotype, which verified Δ2,3 transposase does cause mutations within EF_T.

Discussion

The mutant LF_TDN2 did not produce a protein product that could be detected by Western blotting. In addition, LF_TDN2, when coexpressed with a GST tagged form of LF, decreased expression of LF-GST, indicated through Western blotting showing significantly lower LF levels (Fig. 9d). Taken together, the data suggests this mutant is an RNAi. As my goal was to generate dominant negatives for the purpose of developing toxins, there was no reason to attempt further analysis.

LF_TDN1 did not produce a protein product detectable by Western blotting either, but it also did not cause a reduction of LF-GST. A lack of detectable protein product does not exclude the possibility that LF_TDN1 is a protein-encoding gene. It can be that a protein is produced, but is not stable enough to be detected. Another explanation is that the mutant protein folds in such a way to make the FLAG tag less accessible to the anti-FLAG antibody.

Sequencing LF_TDN1 would determine definitively whether the mutant is an RNAi or encodes a protein. More importantly, if it were the latter, it would lead to knowing the protein sequence. This kind of information may shed more light to the mechanism of LF, including the significance of that particular domain of LF to its function. Furthermore, LF_TDN1 can be cloned and used to produce and extract LF_TDN1 protein to be used in treatment studies.

Considering the potential, further attempts at PCR should be made. Using inverse PCR (iPCR), a method of PCR used to amplify DNA flanked with only a portion of the sequence known, could be attempted⁷⁷. If iPCR methods prove to

be unsuccessful, another possibility would be to narrow down the breakpoint as much as possible with many more primers using the staggered PCR method. The longest LF_TDN1 DNA sequence that can be produced with this method can be used to make a new transgenic line, which can be tested with *wngGAL4>LF2x* for dominant negative activity.

A new approach for a $\Delta 2,3$ screen for EF_T dominant negatives

In the $\Delta 2,3$ screen for EF_T, some of the progeny which expressed only the mutagen-exposed EF_T, showed a phenotype indicating a loss-of-function mutation, verifying that the $\Delta 2,3$ transposase does act on this P element. Despite this, none of the 12 EF_T dominant negative candidates I tested ended up having real dominant negative activity. This is likely to be due to variations in phenotype intensity. The EF stock used has a highly-varied phenotype, making it difficult to determine if a fly showing weak EF wings is weak due to DN activity, or a weakly expressed wild type EF paired with a null mutation, which has a higher probability of occurring. Every couple vials produced one or more candidates, too frequently to be attributed to DN activity. I would have had more candidates if I kept collecting them, but was limited to twelve because of the time it takes to develop each candidate into a stock and individually test their effect on EF. Establishing a *wngGAL4>EF_T* stock, and using this instead of *wngGAL4>EF*, would likely make a more efficient screen as EF_T has a very consistent phenotype, and thus would not produce “false positives” as the screen with *wngGAL4>EF* did.

Materials and Methods

Transgenic *Drosophila* lines

UAS-LF2x/FM7, *UAS-LF3x/FM7*, and *UAS-EF* were described previously⁵⁷. All *UAS-Rab* transgenic lines were generated by H. Bellen and M. Scott⁶¹ and obtained from the Bloomington Stock Center (Bloomington, IN). All crosses for the Rab screen were kept at 25°C and grown under standard conditions. RNAi lines were obtained from Vienna *Drosophila* Stock Center (Vienna, Austria), except for Sec5 RNAi-Trip, which was obtained from Bloomington Stock Center. Crosses for RNAi screen were done at 25°C and grown under standard conditions. Sec15 RNAi and Slmb RNAi were also done at 18°C.

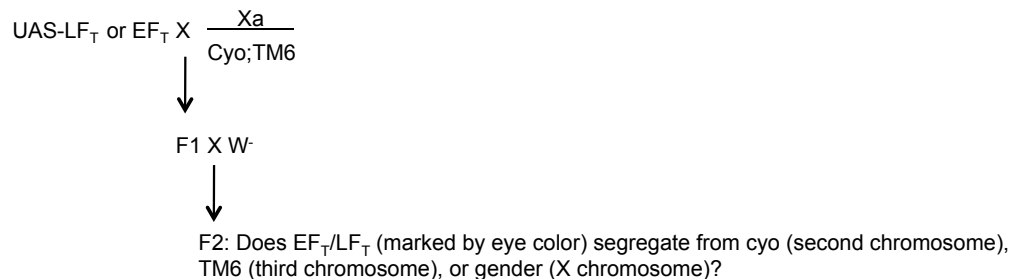
UAS-LF_T and *UAS-EF_T* constructs

LF tagged with Flag and HA (LF_T) and EF tagged with HSV and cMYC (EF_T) (Fig. 7a-b) were made with high-fidelity PCR (Roche) using EF and LF sequences provided by my mentor, Annabel Guichard, and described previously⁵⁷. The following primers were used: LF-Flag sense, 5'-ATAGCGGAT-CCAAAACATGGATTACAAGGACGACGACGACAAGGCGGGCGGTCATGGTG-ATGTAG-3'; LF-HA antisense, 5'-TAATTCAAGTAATAATTGAGTATGGGCA-TGCTGCACGGCCTGATGCGCATCATCAGATCTGCCCTG-3'; EF-HSV sense, 5'-CGATCGGATCCAAAACATGCAGCCGAGCTCGCCCCGAGGATCCAGAA-GATATAGAAGTAAATGCTATGAATGAACATTACA-3'; EF-cMYC antisense, 5'-

GTTTTTTAATAACTACTTTTTCTCGTCTTCGAGTAGAGCCTCCTCCTGGAGA-TTATCTGATCACGCGGC-3.’ Restriction sites for cloning were added to the LF_T and EF_T sequence as part of the primers mentioned above. The LF_T sequence includes a restriction site for BamHI in the N terminus and XbaI in the C terminus. The EF_T sequence has BamHI in the N terminus and SpeI in the C terminus.

The generated PCR products were successfully digested with their respective enzymes and these were cloned using TOPO TA cloning kit (Invitrogen). Cloned LF_T and EF_T, confirmed to be free of significant mutation, were inserted into a pUAST vector modified by Annabel Guichard to contain heat shock (hs). Both UAS-LF_T and UAS-EF_T constructs have a hybrid BamHI/BglII site. The XbaI and SpeI restriction sites remain preserved in the LF_T and EF_T constructs, respectively.

LF_T and EF_T constructs were inserted into *D. melanogaster* with *white*⁻ type background. This was done using Turbo DNA kit and injecting into fly embryos ≤30 minutes old. Transformed flies were identified by their orange-red eye color. The chromosomes UAS-LF_T and UAS-EF_T were inserted into was determined by the following cross-scheme:



The UAS-LF_T insertion was found to be on the third chromosome and homozygous lethal. I generated a UAS-LF_T heterozygous stock with the third chromosome balancer TM3Sb (a balancer which is marked by a stubby hair phenotype). The UAS-EF_T insertion is on the second chromosome and a homozygous stock.

The same cross scheme was used to determine the location of UAS-LF_TDN1 and UAS-LF_TDN2. Both mutants remained on the third chromosome. UAS-LF_TDN1 and UAS-LF_TDN2 were balanced over TM3Sb and TM6, respectively.

Immunofluoresence of wing discs and Western Blotting

Stains for Figure 3, are previously described¹⁷. Antibodies used for images in Figure 4 are: rat anti-DECad (1:500), mouse anti- Delta (1:500), mouse anti-Rab11 (1:200) (Biosciences). Antibodies used in Western blotting are: rabbit anti-FLAG (1:200) (Sigma) followed by chicken anti-rabbit Alexa Fluor 488; rat anti-HA (1:1000) followed by chicken anti-rat Alexa Fluor 647; rabbit anti-GST (1:1000) followed by chicken anti-rabbit Alexa Fluor 488.

DNA analysis of LF_TDN1 and LF_TDN2

PCR reactions were done using *Taq* PCR Master Mix (Qiagen), using the following primers: LF1 sense, 5'-ACGAAATAAAACACAGGAAGAGCATTT-3'; LF4 antisense, 5'-GCATAAAGCTGTAAACATCACGATGC-3'; LF10 antisense, 5'-CCTCACTATCATTCCTTAATTCTACACC-3.'

Supplementary Tables

Supplementary Table 1: Effects of expressing dominant negative Rabs (RabDN) in the wing and the effects of wild-type Rabs (RabWT) on EF phenotype. RabDNs and RabWTs were expressed with wngG4 and RabWTs were also coexpressed with EF. Only Rab11(DN) mimicked the EF phenotype, and only Rab(WT) had the ability to suppress the EF phenotype

Rab protein	BL# for RabDN	Wing phenotype in wngG4>RabDN	BL# for RabWT	Wing phenotype in wngG4>Rabwt	Wing phenotype in wngG4>EF+Rabwt
Rab1	9757	100% lethal	24104	No phenotype	Semi lethal
Rab2	9759	No phenotype	23246	No phenotype	No effect on EF
Rab3	9766	No phenotype	9762	No phenotype	No effect on EF
Rab4	9768, 9769	No phenotype	23269 9767	No phenotype	No effect on EF
Rab5	9771, 9772	100% lethal	9775 24616	No phenotype	No effect on EF
Rab6	23249	No phenotype	23251	No phenotype	No effect on EF
Rab7	9778	No phenotype	23641	No phenotype	Mild enhancement of EF phenotype
Rab8	23271	No phenotype	23272	No phenotype	No effect on EF
Rab9	23642	No phenotype	9783	No phenotype	No effect on EF
Rab10	9788	No phenotype	9789	Weak curvature	No effect on EF
Rab11	9792	EF-like phenotype	9790	No phenotype	Suppression of EF phenotype
Rab14	23263	L2 and L3 thicker and closer than normal. Extra vein tissue.	9793 9794	No phenotype	No effect on EF
Rab18	23237	No phenotype	9796	No phenotype	Milder EF phenotype
Rab19	9799	No phenotype	24150	No phenotype	Enhancement
Rab21	23240	No phenotype	23242	Weak EF-like phenotype	Enhanced EF phenotype
Rab23	9804	No phenotype	9802	No phenotype	No effect on EF
Rab26	9807	No phenotype	23244	No phenotype	No effect on EF
Rab27	23267	No phenotype	9810	No phenotype	No effect on EF
Rab30	9813	No phenotype	9812	No phenotype	No effect on EF
Rab32	23281	No phenotype	23282	No phenotype	No effect on EF
Rab35	9819	Curved wings	9821	No phenotype	No effect on EF
Rab39	23247	No phenotype	9825	Lethal in males, Weak curvature	Weak enhancement of EF phenotype
Rab40	9828	Curved wings	9830	No phenotype	No effect on EF
RabX1	9838	No phenotype	23274	No phenotype	No effect on EF
RabX2	9843	No phenotype	23275	No phenotype	Enhancement of EF phenotype
RabX3	9845	No phenotype	23276	No phenotype	No effect on EF
RabX4	9849	No phenotype	9851	No phenotype	No effect on EF
RabX5	9853	No phenotype	9854	No phenotype	No effect on EF
RabX6	23253	No phenotype	23278	No phenotype	No effect on EF




Supplementary Table 2: Wing phenotypes of RNAi lines and their effects on EF and LF phenotype. All crosses were done at 25°C. Few were repeated at 18°C. These are noted with “(18°C)” next to the gene.

KEY:







↑	Strong enhancement of phenotype, likely synergy
↑	Enhancement of phenotype
↑	Possible enhancement
↓	Milder phenotype
↓	Possible decrease in phenotype
⊖	no effect
L	lethal
IC	inconclusive

In some cases, the RNAi itself produced a strong-severe phenotype which dominated over the EF and LF phenotypes. In these cases, the effect designated in the +EF or +LF column, compares to the RNAi phenotype and is designated by ^{RNAi} next to the symbol. For example, ↓^{RNAi} in the +EF column for Sec3^{RNAi} means that coexpression of Sec3^{RNAi} is milder than Sec3^{RNAi} alone, not milder than EF.

* Is expressed with VgGAL4, which expresses along the margin. All others are with wngGAL4.






	GD/KK# or BL#	Gene	RNAi expressed with MS1096Gal4	+EF	+LF
Core Exocyst Components	KK108085	Sec3 ^{RNAi}		↓ ^{RNAi}	≈ to RNAi
	GD 28873/288 74	Sec5 ^{RNAi}	Refer to Figure 4c	⊖	↑
	BL#27526	Sec5 ^{RNAi-TRIP}	Refer to Figure 4e	↓ ^{RNAi}	↑
	KK105836	Sec6 ^{RNAi}		↓ ^{RNAi}	≈ to RNAi
	KK10178	Sec15 ^{RNAi} (18°C)	Refer to Figure 4a	≈	↑
	KK101154	Exo70 ^{RNAi}	Refer to Figure 4g	↑	↑
	KK108650	Exo84 ^{RNAi}		↓ ^{RNAi}	↓ ^{RNAi}

Supplementary Table 2: Wing phenotypes of RNAi lines and their effects on EF and LF phenotype. Table continued






Components of Exocyst Pathway	KK109420	Rho1 ^{RNAi}		I/C	L
	KK104675	Rok ^{RNAi}		[1] ↑	↑
	KK110213	RhoGAPp190 ^{RNAi}	No phenotype	⊖	⊖
	KK107825	Slmb (18°C)		↓	↓
Rab11 Adjacent Genes	KK108213	Ppan ^{RNAi}		↑	≈ to RNAi+EF
	KK110473	VgG4>Ppan ^{RNAi}		N/A	N/A
		Rtet ^{RNAi}		↑	↑

[1] “growths” seen in rok^{RNAi} nearly completely disappear with EF and LF






Supplementary Table 2: Wing phenotypes of RNAi lines and their effects on EF and LF phenotype. Table continued

	KK100136	Rhogap93B ^{RNAi}		↑	↑
	KK100028	CG17282 ^{RNAi}	Refer to fig #	↑	↑
	KK108659	CG5745 ^{RNAi}	Refer to Fig #	↑	↑
	GD27812	CG7044 ^{RNAi}	No phenotype	↓	↓
	KK108209	Snap24 ^{RNAi}		↑	↑
Trafficking	KK100608	synaptotagmin ^{RNAi}		↑	↑
	KK109604	l(2)gl ^{RNAi}		L	↑
Membrane					
Cytoskeletal protein	KK103962	DECad ^{RNAi} (18°C)		↑ ^{RNAi}	≈ to RNAi L
Adhe	KK102686	canoe ^{RNAi}	No phenotype	⊖	⊖
	GD38863	polychaetoid ^{RNAi}	No phenotype	IC	↑
	KK109274	dlg ^{RNAi}	No phenotype	⊖	⊖

Supplementary Table 2: Wing phenotypes of RNAi lines and their effects on EF and LF phenotype. Table continued

	KK104279	echinoid ^{RNAi}		↑	↑
	9446-R	coro ^{RNAi}		↓	⊖
	GD50307	pck ^{RNAi} (megatrachea)	No phenotype	⊖	⊖
Septate Junction Proteins	GD44929	Sinuous ^{RNAi}	Curved, scrunched	↑	↑
	KK108224	Kune-kune ^{RNAi}		↑	↑
	KK107991	nrg ^{RNAi}		↑	↑
	GD50372	Epac ^{RNAi}	No phenotype	↓	IC
	GD27017	Dizzy ^{RNAi}	Very mild phenotype. Some slight downward curve in males	⊖	↑
	KK101524	PKA-C1 ^{RNAi}		↑	↑
Δ	KK108424	PKA-C2 ^{RNAi}	No phenotype	↓	⊖

Supplementary Table 2: Wing phenotypes of RNAi lines and their effects on EF and LF phenotype. Table continued

	KK101763	PKA-R2 ^{RNAi}		↑	↑
	KK107056	rugose ^{RNAi}		↑	↑
	KK105107	yu ^{RNAi}	No phenotype	⊖	IC
	KK100273	nervy ^{RNAi}	Smaller, rounder, bowl-like curve, "pinch" at proximal part of wing	⊖	↑
	KK102374	AKAP200 ^{RNAi}		↑	
	GD105296	rai ^{RNAi}	Curly, scrunched	IC	IC
	KK107967	dunce ^{RNAi}	No phenotype	⊖	⊖
	KK101759	rut ^{RNAi}	No phenotype	⊖	↑
	KK109860	Arrestin1 ^{RNAi}	Extremely mild phenotype Slight curve around margin	⊖	↑
	KK100685	stardust ^{RNAi}		⊖	↑
	KK109413	CG15609 ^{RNAi}		≈ to CG1560 ^{RNAi} ↓ ^{RNAi}	≈ to CG1560 ^{RNAi} ↓ ^{RNAi}

References

1. Pasteur, L., Chamberland, C. & Roux, E. Summary report of the experiments conducted at Pouilly-le-Fort, near Melun, on the anthrax vaccination, 1881. *Yale J. Biol. Med.* **75**, 59–62 (2002).
2. Metcalfe, N. The history of woolsorters' disease: a Yorkshire beginning with an international future? *Occup. Med. Oxf. Engl.* **54**, 489–493 (2004).
3. Chitlaru, T., Altboum, Z., Reuveny, S. & Shafferman, A. Progress and novel strategies in vaccine development and treatment of anthrax. *Immunol. Rev.* **239**, 221–236 (2011).
4. Jernigan, D. B., Raghunathan, P. L., Bell, B. P., Brechner, R., Bresnitz, E. A., Butler, J. C., Cetron, M., Cohen, M., Doyle, T., Fischer, M., Greene, C., Griffith, K. S., Guarner, J., Hadler, J. L., Hayslett, J. A., Meyer, R., Petersen, L. R., Phillips, M., Pinner, R., Popovic, T., Quinn, C. P., Reefhuis, J., Reissman, D., Rosenstein, N., Schuchat, A., Shieh, W.-J., Siegal, L., Swerdlow, D. L., Tenover, F. C., Traeger, M., Ward, J. W., Weisfuse, I., Wiersma, S., Yeskey, K., Zaki, S., Ashford, D. A., Perkins, B. A., Ostroff, S., Hughes, J., Fleming, D., Koplan, J. P., Gerberding, J. L. & the National Anthrax Epidemiologic Investigation Team. Investigation of Bioterrorism-Related Anthrax, United States, 2001: Epidemiologic Findings. *Emerg. Infect. Dis.* **8**, 1019–1028 (2002).
5. Zilinskas, R. A. Iraq's biological weapons. The past as future? *Jama J. Am. Med. Assoc.* **278**, 418–424 (1997).
6. Guichard, A., Nizet, V. & Bier, E. New insights into the biological effects of anthrax toxins: linking cellular to organismal responses. *Microbes Infect. Inst. Pasteur* **14**, 97–118 (2012).
7. Chakraborty, P. P., Thakurt, S. G., Satpathi, P. S., Hansda, S., Sit, S., Achar, A. & Banerjee, D. Outbreak of cutaneous anthrax in a tribal village: a clinico-epidemiological study. *J. Assoc. Physicians India* **60**, 89–93 (2012).
8. Knox, D., Murray, G., Millar, M., Hamilton, D., Connor, M., Ferdinand, R. D. & Jones, G. A. Subcutaneous anthrax in three intravenous drug users: a new clinical diagnosis. *J. Bone Joint Surg. Br.* **93**, 414–417 (2011).
9. Ramsay, C. N., Stirling, A., Smith, J., Hawkins, G., Brooks, T., Hood, J., Penrice, G., Browning, L. M. & Ahmed, S. An outbreak of infection with *Bacillus anthracis* in injecting drug users in Scotland. *Euro Surveill. Bull. Eur. Sur Mal. Transm. Eur. Commun. Dis. Bull.* **15**, (2010).
10. Holzmann, T., Frangoulidis, D., Simon, M., Noll, P., Schmoldt, S., Hanczaruk, M., Grass, G., Pregler, M., Sing, A., Hörmansdorfer, S., Bernard, H., Grunow, R., Zimmermann, R., Schneider-Brachert, W., Gessner, A. & Reischl, U. Fatal

- anthrax infection in a heroin user from southern Germany, June 2012. *Euro Surveill. Bull. Eur. Sur Mal. Transm. Eur. Commun. Dis. Bull.* **17**, (2012).
11. Hang'ombe, M. B., Mwansa, J. C. L., Muwowo, S., Mulenga, P., Kapina, M., Musenga, E., Squarre, D., Mataa, L., Thomas, S. Y., Ogawa, H., Sawa, H. & Higashi, H. Human-animal anthrax outbreak in the Luangwa valley of Zambia in 2011. *Trop. Doct.* **42**, 136–139 (2012).
 12. Gombe, N., Nkomo, B., Chadambuka, A., Shambira, G. & Tshimanga, M. Risk factors for contracting anthrax in Kuwirirana ward, Gokwe North, Zimbabwe. *Afr. Health Sci.* **10**, 159–164 (2010).
 13. Doganay, M. & Metan, G. Human Anthrax in Turkey from 1990 to 2007. *Vector-Borne Zoonotic Dis.* **9**, 131–140 (2009).
 14. Guarner, J., Jernigan, J. A., Shieh, W.-J., Tatti, K., Flannagan, L. M., Stephens, D. S., Popovic, T., Ashford, D. A., Perkins, B. A. & Zaki, S. R. Pathology and pathogenesis of bioterrorism-related inhalational anthrax. *Am. J. Pathol.* **163**, 701–709 (2003).
 15. Lowe, D. E. & Glomski, I. J. Cellular and Physiological Effects of Anthrax Exotoxin and Its Relevance to Disease. *Front. Cell. Infect. Microbiol.* **2**, (2012).
 16. Abramova, F. A., Grinberg, L. M., Yampolskaya, O. V. & Walker, D. H. Pathology of inhalational anthrax in 42 cases from the Sverdlovsk outbreak of 1979. *Proc. Natl. Acad. Sci. U. S. A.* **90**, 2291–2294 (1993).
 17. Guichard, A., McGillivray, S. M., Cruz-Moreno, B., van Sorge, N. M., Nizet, V. & Bier, E. Anthrax toxins cooperatively inhibit endocytic recycling by the Rab11/Sec15 exocyst. *Nature* **467**, 854–858 (2010).
 18. Bolcome, R. E., 3rd, Sullivan, S. E., Zeller, R., Barker, A. P., Collier, R. J. & Chan, J. Anthrax lethal toxin induces cell death-independent permeability in zebrafish vasculature. *Proc. Natl. Acad. Sci. U. S. A.* **105**, 2439–2444 (2008).
 19. Moayeri, M., Crown, D., Dorward, D. W., Gardner, D., Ward, J. M., Li, Y., Cui, X., Eichacker, P. & Leppla, S. H. The heart is an early target of anthrax lethal toxin in mice: a protective role for neuronal nitric oxide synthase (nNOS). *Plos Pathog.* **5**, e1000456 (2009).
 20. Lawrence, W. S., Marshall, J. R., Zavala, D. L., Weaver, L. E., Baze, W. B., Moen, S. T., Whorton, E. B., Gourley, R. L. & Peterson, J. W. Hemodynamic Effects of Anthrax Toxins in the Rabbit Model and the Cardiac Pathology Induced by Lethal Toxin. *Toxins* **3**, 721–736 (2011).
 21. Firoved, A. M., Miller, G. F., Moayeri, M., Kakkar, R., Shen, Y., Wiggins, J. F., McNally, E. M., Tang, W.-J. & Leppla, S. H. *Bacillus anthracis* edema toxin causes extensive tissue lesions and rapid lethality in mice. *Am. J. Pathol.* **167**, 1309–1320 (2005).

22. Koch, R. Die Ätiologie der Milzbrand-Krankheit, begründet auf die Entwicklungsgeschichte des *Bacillus anthracis*. *Cohns Beitrage Zur Biol. Pflanz.* (1876).
23. Green, Brian D., Battisti, Laurie, Koehler, Theresa M., Thorne, Curtis B. & Ivins, Bruce E. Demonstration of a Capsule Plasmid in *Bacillus anthracis*. *Infect. Immun.* **49**, 291–297 (1985).
24. Mikesell, P., Ivins, B. E., Ristoph, J. D. & Dreier, T. M. Evidence for plasmid-mediated toxin production in *Bacillus anthracis*. *Infect. Immun.* **39**, 371–376 (1983).
25. Okinaka, R. T., Cloud, K., Hampton, O., Hoffmaster, A. R., Hill, K. K., Keim, P., Koehler, T. M., Lamke, G., Kumano, S., Mahillon, J., Manter, D., Martinez, Y., Ricke, D., Svensson, R. & Jackson, P. J. Sequence and organization of pXO1, the large *Bacillus anthracis* plasmid harboring the anthrax toxin genes. *J. Bacteriol.* **181**, 6509–6515 (1999).
26. Bradley, K. A., Mogridge, J., Mourez, M., Collier, R. J. & Young, J. A. Identification of the cellular receptor for anthrax toxin. *Nature* **414**, 225–229 (2001).
27. Scobie, H. M., Rainey, G. J. A., Bradley, K. A. & Young, J. A. T. Human capillary morphogenesis protein 2 functions as an anthrax toxin receptor. *Proc. Natl. Acad. Sci. U. S. A.* **100**, 5170–5174 (2003).
28. Klimpel, K. R., Molloy, S. S., Thomas, G. & Leppla, S. H. Anthrax toxin protective antigen is activated by a cell surface protease with the sequence specificity and catalytic properties of furin. *Proc. Natl. Acad. Sci. U. S. A.* **89**, 10277–10281 (1992).
29. Gordon, V. M., Klimpel, K. R., Arora, N., Henderson, M. A. & Leppla, S. H. Proteolytic activation of bacterial toxins by eukaryotic cells is performed by furin and by additional cellular proteases. *Infect. Immun.* **63**, 82–87 (1995).
30. Milne, J. C., Furlong, D., Hanna, P. C., Wall, J. S. & Collier, R. J. Anthrax protective antigen forms oligomers during intoxication of mammalian cells. *J. Biol. Chem.* **269**, 20607–20612 (1994).
31. Mogridge, J., Cunningham, K. & Collier, R. J. Stoichiometry of anthrax toxin complexes. *Biochemistry (Mosc.)* **41**, 1079–1082 (2002).
32. Mogridge, J., Cunningham, K., Lacy, D. B., Mourez, M. & Collier, R. J. The lethal and edema factors of anthrax toxin bind only to oligomeric forms of the protective antigen. *Proc. Natl. Acad. Sci. U. S. A.* **99**, 7045–7048 (2002).
33. Abrami, L., Liu, S., Cosson, P., Leppla, S. H. & van der Goot, F. G. Anthrax toxin triggers endocytosis of its receptor via a lipid raft-mediated clathrin-dependent process. *J. Cell Biol.* **160**, 321–328 (2003).

34. Koehler, T. M. & Collier, R. J. Anthrax toxin protective antigen: low-pH-induced hydrophobicity and channel formation in liposomes. *Mol. Microbiol.* **5**, 1501–1506 (1991).
35. Miller, C. J., Elliott, J. L. & Collier, R. J. Anthrax protective antigen: prepore-to-pore conversion. *Biochemistry (Mosc.)* **38**, 10432–10441 (1999).
36. Abrami, L., Lindsay, M., Parton, R. G., Leppla, S. H. & van der Goot, F. G. Membrane insertion of anthrax protective antigen and cytoplasmic delivery of lethal factor occur at different stages of the endocytic pathway. *J. Cell Biol.* **166**, 645–651 (2004).
37. Zorretta, I., Brandi, L., Janowiak, B., Dal Molin, F., Tonello, F., Collier, R. J. & Montecucco, C. Imaging the cell entry of the anthrax oedema and lethal toxins with fluorescent protein chimeras. *Cell. Microbiol.* **12**, 1435–1445 (2010).
38. Guidi-Rontani, C., Weber-Levy, M., Mock, M. & Cabiaux, V. Translocation of *Bacillus anthracis* lethal and oedema factors across endosome membranes. *Cell. Microbiol.* **2**, 259–264 (2000).
39. Leppla, S. H. Anthrax toxin edema factor: a bacterial adenylate cyclase that increases cyclic AMP concentrations of eukaryotic cells. *Proc. Natl. Acad. Sci. U. S. A.* **79**, 3162–3166 (1982).
40. Tang, W.-J. & Guo, Q. The adenylyl cyclase activity of anthrax edema factor. *Mol. Aspects Med.* **30**, 423–430 (2009).
41. Dal Molin, F., Tonello, F., Ladant, D., Zorretta, I., Zamparo, I., Di Benedetto, G., Zaccolo, M. & Montecucco, C. Cell entry and cAMP imaging of anthrax edema toxin. *Embo J.* **25**, 5405–5413 (2006).
42. De Rooij, J., Zwartkruis, F. J., Verheijen, M. H., Cool, R. H., Nijman, S. M., Wittinghofer, A. & Bos, J. L. Epac is a Rap1 guanine-nucleotide-exchange factor directly activated by cyclic AMP. *Nature* **396**, 474–477 (1998).
43. Borland, G., Smith, B. O. & Yarwood, S. J. EPAC proteins transduce diverse cellular actions of cAMP. *Br. J. Pharmacol.* **158**, 70–86 (2009).
44. Duesbery, N. S., Webb, C. P., Leppla, S. H., Gordon, V. M., Klimpel, K. R., Copeland, T. D., Ahn, N. G., Oskarsson, M. K., Fukasawa, K., Paull, K. D. & Vande Woude, G. F. Proteolytic inactivation of MAP-kinase-kinase by anthrax lethal factor. *Science* **280**, 734–737 (1998).
45. Pellizzari, R., Guidi-Rontani, C., Vitale, G., Mock, M. & Montecucco, C. Anthrax lethal factor cleaves MKK3 in macrophages and inhibits the LPS/IFN γ -induced release of NO and TNF α . *Febs Lett.* **462**, 199–204 (1999).
46. Vitale, G., Bernardi, L., Napolitani, G., Mock, M. & Montecucco, C. Susceptibility of mitogen-activated protein kinase kinase family members to proteolysis by anthrax lethal factor. *Biochem. J.* **352 Pt 3**, 739–745 (2000).

47. Dérjard, B., Raingeaud, J., Barrett, T., Wu, I. H., Han, J., Ulevitch, R. J. & Davis, R. J. Independent human MAP-kinase signal transduction pathways defined by MEK and MKK isoforms. *Science* **267**, 682–685 (1995).
48. Quinn, C. P., Singh, Y., Klimpel, K. R. & Leppla, S. H. Functional mapping of anthrax toxin lethal factor by in-frame insertion mutagenesis. *J. Biol. Chem.* **266**, 20124–20130 (1991).
49. Pannifer, A. D., Wong, T. Y., Schwarzenbacher, R., Renatus, M., Petosa, C., Bienkowska, J., Lacy, D. B., Collier, R. J., Park, S., Leppla, S. H., Hanna, P. & Liddington, R. C. Crystal structure of the anthrax lethal factor. *Nature* **414**, 229–233 (2001).
50. Stanley, J. L. & Smith, H. Purification of factor I and recognition of a third factor of the anthrax toxin. *J. Gen. Microbiol.* **26**, 49–63 (1961).
51. Pezard, C., Berche, P. & Mock, M. Contribution of individual toxin components to virulence of *Bacillus anthracis*. *Infect. Immun.* **59**, 3472–3477 (1991).
52. Gladstone, G. Immunity to Anthrax: Protective Antigen Present in Cell-Free Culture Filtrates. *Br J Exp Pathol* **27**, 394–418 (1946).
53. Altboum, Z., Gozes, Y., Barnea, A., Pass, A., White, M. & Kobiler, D. Postexposure prophylaxis against anthrax: evaluation of various treatment regimens in intranasally infected guinea pigs. *Infect. Immun.* **70**, 6231–6241 (2002).
54. Hicks, C. W., Cui, X., Sweeney, D. A., Li, Y., Barochia, A. & Eichacker, P. Q. The potential contributions of lethal and edema toxins to the pathogenesis of anthrax associated shock. *Toxins (Basel)* **3**, 1185–1202 (2011).
55. Bier, E. *Drosophila*, the golden bug, emerges as a tool for human genetics. *Nat. Rev. Genet.* **6**, 9–23 (2005).
56. Brand, A. H. & Perrimon, N. Targeted gene expression as a means of altering cell fates and generating dominant phenotypes. *Dev. Camb. Engl.* **118**, 401–415 (1993).
57. Guichard, A., Park, J. M., Cruz-Moreno, B., Karin, M. & Bier, E. Anthrax lethal factor and edema factor act on conserved targets in *Drosophila*. *Proc. Natl. Acad. Sci. U. S. A.* **103**, 3244–3249 (2006).
58. Guruharsha, K. G., Kankel, M. W. & Artavanis-Tsakonas, S. The Notch signalling system: recent insights into the complexity of a conserved pathway. *Nat. Rev. Genet.* **13**, 654–666 (2012).
59. Musse, A. A., Meloty-Kapella, L. & Weinmaster, G. Notch ligand endocytosis: mechanistic basis of signaling activity. *Semin. Cell Dev. Biol.* **23**, 429–436 (2012).
60. Stenmark, H. Rab GTPases as coordinators of vesicle traffic. *Nat. Rev. Mol. Cell Biol.* **10**, 513–525 (2009).

61. Zhang, J., Schulze, K. L., Hiesinger, P. R., Suyama, K., Wang, S., Fish, M., Acar, M., Hoskins, R. A., Bellen, H. J. & Scott, M. P. Thirty-one flavors of *Drosophila* rab proteins. *Genetics* **176**, 1307–1322 (2007).
62. Zhang, X.-M., Ellis, S., Sriratanana, A., Mitchell, C. A. & Rowe, T. Sec15 is an effector for the Rab11 GTPase in mammalian cells. *J. Biol. Chem.* **279**, 43027–43034 (2004).
63. Donlin, M. J. in *Curr. Protoc. Bioinforma.* (Baxevanis, A. D., Page, R. D. M., Petsko, G. A., Stein, L. D. & Stormo, G. D.) (John Wiley & Sons, Inc., 2009). at <<http://doi.wiley.com/10.1002/0471250953.bi0909s28>>
64. Altschul, S. F., Gish, W., Miller, W., Myers, E. W. & Lipman, D. J. Basic local alignment search tool. *J. Mol. Biol.* **215**, 403–410 (1990).
65. Ketting, R. F., Fischer, S. E., Bernstein, E., Sijen, T., Hannon, G. J. & Plasterk, R. H. Dicer functions in RNA interference and in synthesis of small RNA involved in developmental timing in *C. elegans*. *Genes Dev.* **15**, 2654–2659 (2001).
66. Langevin, J., Morgan, M. J., Sibarita, J.-B., Aresta, S., Murthy, M., Schwarz, T., Camonis, J. & Bellaïche, Y. *Drosophila* exocyst components Sec5, Sec6, and Sec15 regulate DE-Cadherin trafficking from recycling endosomes to the plasma membrane. *Dev. Cell* **9**, 365–376 (2005).
67. Fortini, M. E. & Bilder, D. Endocytic regulation of Notch signaling. *Curr. Opin. Genet. Dev.* **19**, 323–328 (2009).
68. Ren, J. & Guo, W. ERK1/2 regulate exocytosis through direct phosphorylation of the exocyst component Exo70. *Dev. Cell* **22**, 967–978 (2012).
69. Chang, L. & Karin, M. Mammalian MAP kinase signalling cascades. *Nature* **410**, 37–40 (2001).
70. Bernards, A. GAPs galore! A survey of putative Ras superfamily GTPase activating proteins in man and *Drosophila*. *Biochim. Biophys. Acta Bba - Rev. Cancer* **1603**, 47–82 (2003).
71. Ortiz, D., Medkova, M., Walch-Solimena, C. & Novick, P. Ypt32 recruits the Sec4p guanine nucleotide exchange factor, Sec2p, to secretory vesicles; evidence for a Rab cascade in yeast. *J. Cell Biol.* **157**, 1005–1015 (2002).
72. Nottingham, R. M. & Pfeffer, S. R. Defining the boundaries: Rab GEFs and GAPs. *Proc. Natl. Acad. Sci.* **106**, 14185–14186 (2009).
73. Hurst, L. D., Pál, C. & Lercher, M. J. The evolutionary dynamics of eukaryotic gene order. *Nat. Rev. Genet.* **5**, 299–310 (2004).
74. Crow, J. F. in *Mutat. Cancer Malform.* (Chu, E. H. Y. & Generoso, W. M.) 257–273 (Springer US, 1984). at <http://www.springerlink.com/index/10.1007/978-1-4613-2399-0_13>

75. Delattre, M., Anxolabéhère, D. & Coen, D. Prevalence of localized rearrangements vs. transpositions among events induced by Drosophila P element transposase on a P transgene. *Genetics* **141**, 1407–1424 (1995).
76. Guichard, A., Srinivasan, S., Zimm, G. & Bier, E. A screen for dominant mutations applied to components in the Drosophila EGF-R pathway. *Proc. Natl. Acad. Sci. U. S. A.* **99**, 3752–3757 (2002).
77. Huang, A. M., Rehm, E. J. & Rubin, G. M. Recovery of DNA sequences flanking P-element insertions in Drosophila: inverse PCR and plasmid rescue. *Cold Spring Harb. Protoc.* **2009**, pdb.prot5199 (2009).